Today's outline - March 03, 2020

Today's outline - March 03, 2020

- Crystal truncation rods

Today's outline - March 03, 2020

- Crystal truncation rods
- Diffuse Scattering

Today's outline - March 03, 2020

- Crystal truncation rods
- Diffuse Scattering
- Modulated structures

Today's outline - March 03, 2020

- Crystal truncation rods
- Diffuse Scattering
- Modulated structures
- Lattice vibrations

Today's outline - March 03, 2020

- Crystal truncation rods
- Diffuse Scattering
- Modulated structures
- Lattice vibrations

Homework Assignment #04:
Chapter 4: 2, 4, 6, 7, 10
due Tuesday, March 10, 2020

Hydrated surface of magnetite

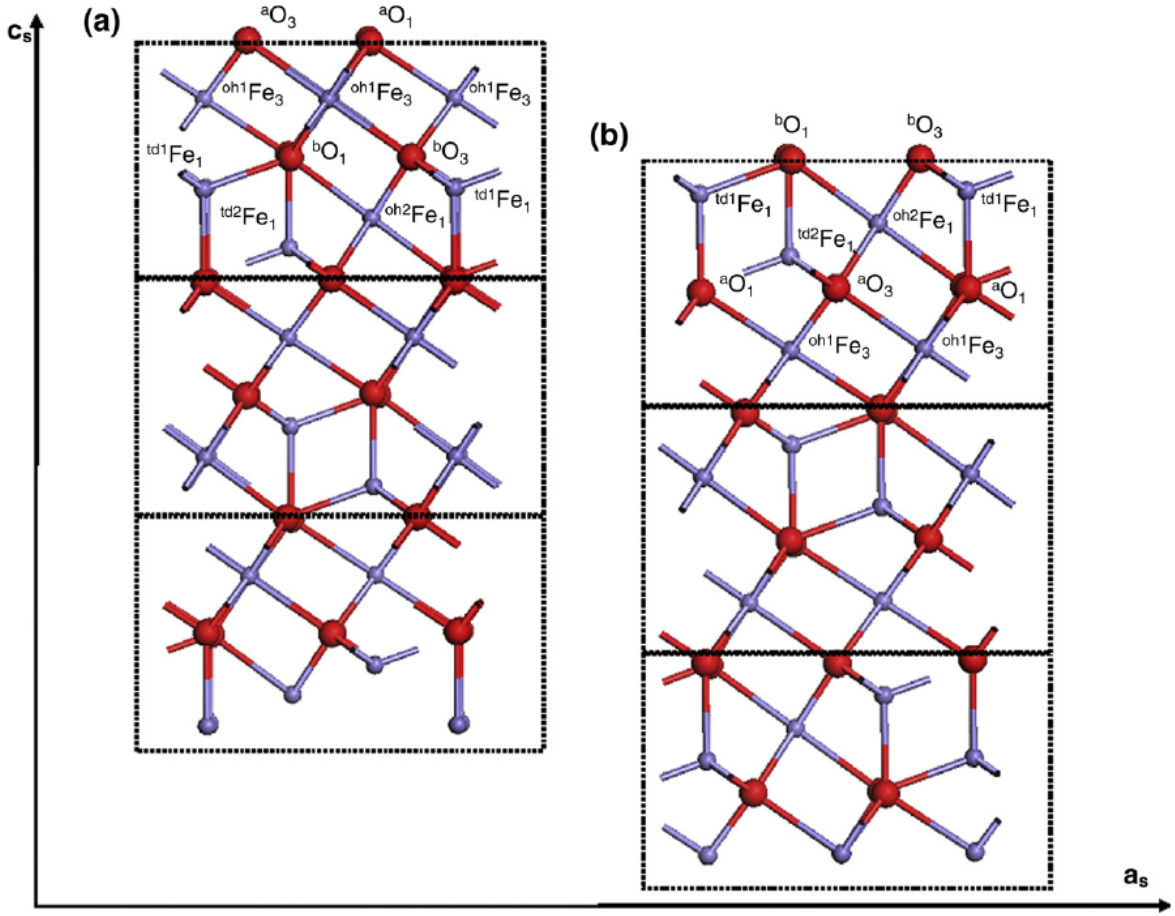

"Surface structure of magnetite (111) under hydrated conditions by crystal truncation rod diffraction," S.C. petitto et al. *Surf. Sci.* **604**, 1082-1093 (2010).

Hydrated surface of magnetite

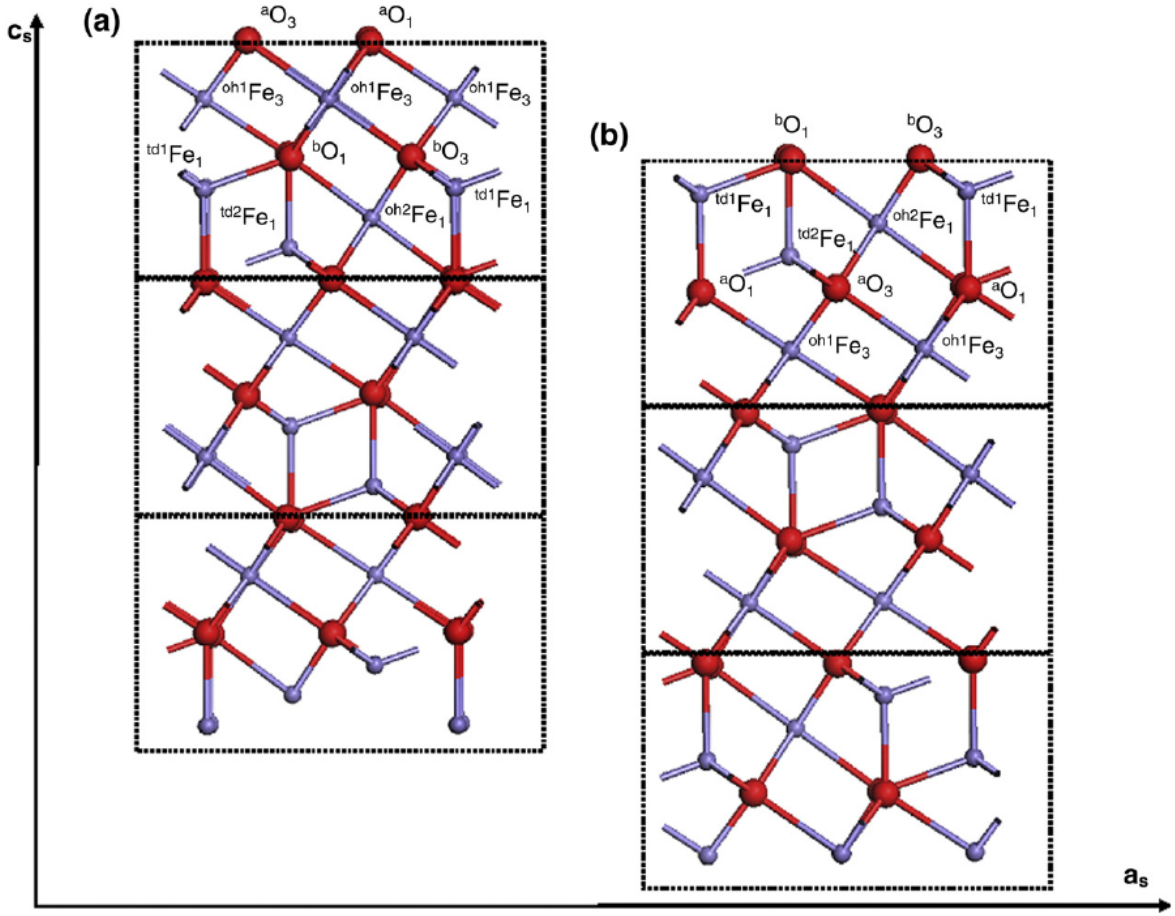

Magnetite, Fe_3O_4, is a technologically important material for environmental remediation

"Surface structure of magnetite (111) under hydrated conditions by crystal truncation rod diffraction," S.C. petitto et al. *Surf. Sci.* **604**, 1082-1093 (2010).

Hydrated surface of magnetite

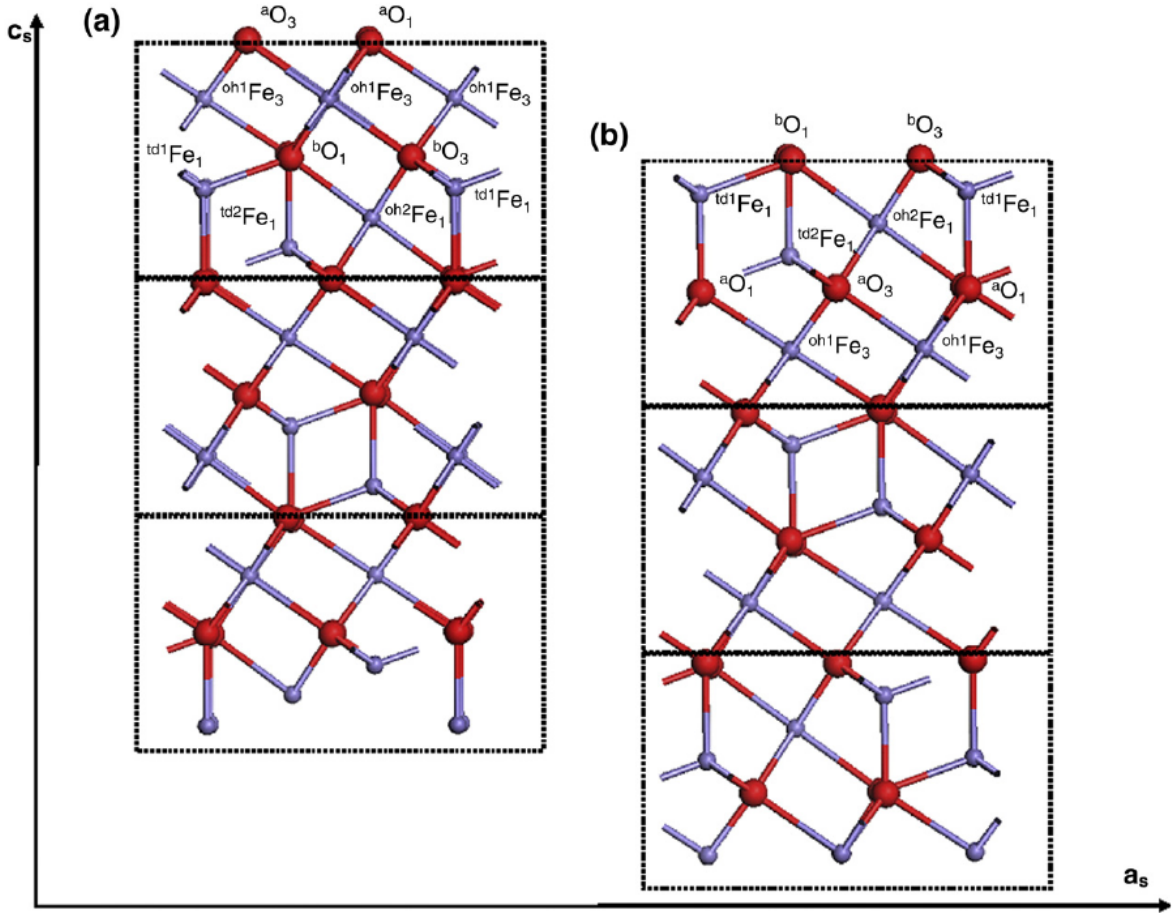

Magnetite, Fe_3O_4, is a technologically important material for environmental remediation

It is important to know the structure of the surface of magnetite in a hydrated environment to understand the processes that favor sorption of heavy elements

"Surface structure of magnetite (111) under hydrated conditions by crystal truncation rod diffraction," S.C. petitto et al. *Surf. Sci.* **604**, 1082-1093 (2010).

Hydrated surface of magnetite

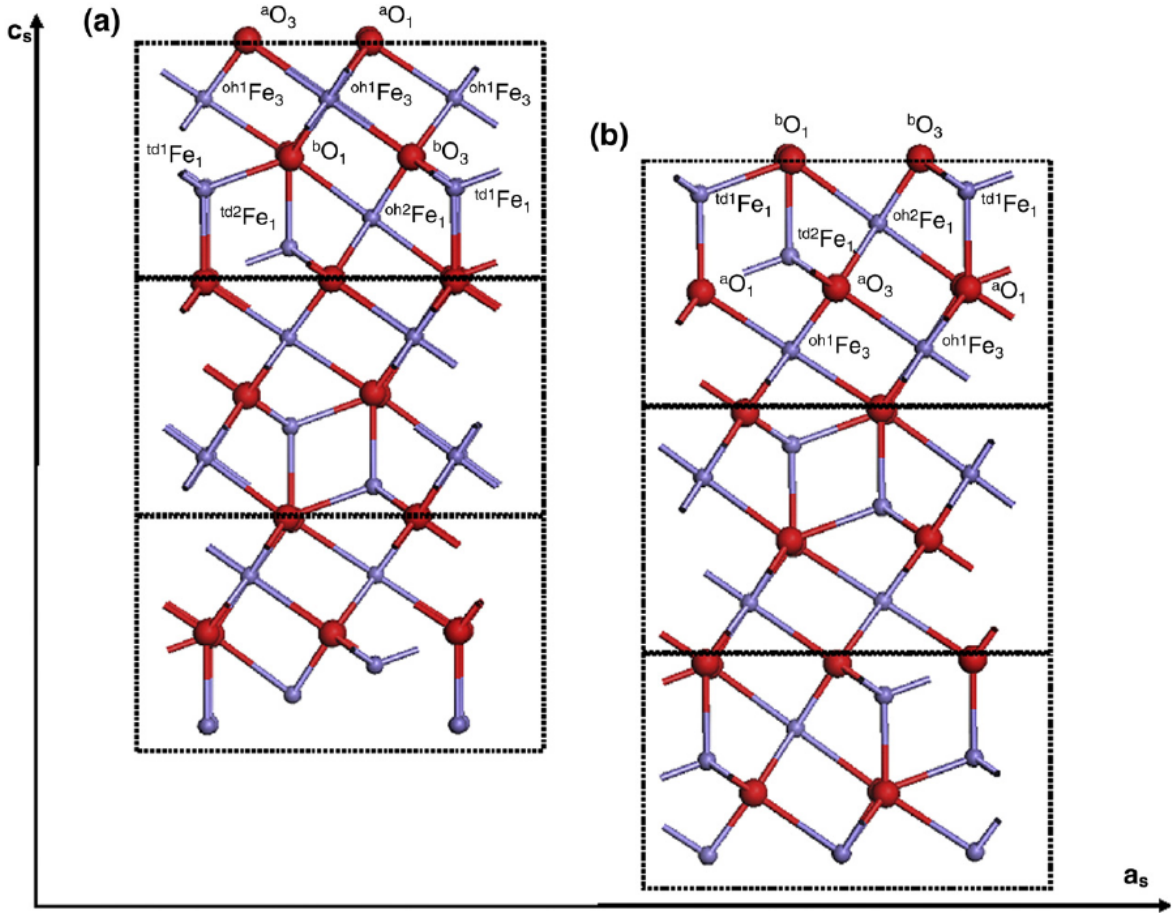

Magnetite, Fe_3O_4, is a technologically important material for environmental remediation

It is important to know the structure of the surface of magnetite in a hydrated environment to understand the processes that favor sorption of heavy elements

There are two possible surfaces, the oxygen octahedral iron, OOI (a), and the oxygen mixed-iron, OMI (b), terminations

"Surface structure of magnetite (111) under hydrated conditions by crystal truncation rod diffraction," S.C. petitto et al. *Surf. Sci.* **604**, 1082-1093 (2010).

Magnetite (111) surface

Crystal truncation rod measurements require an oriented single crystal with a polished and cleaned surface.

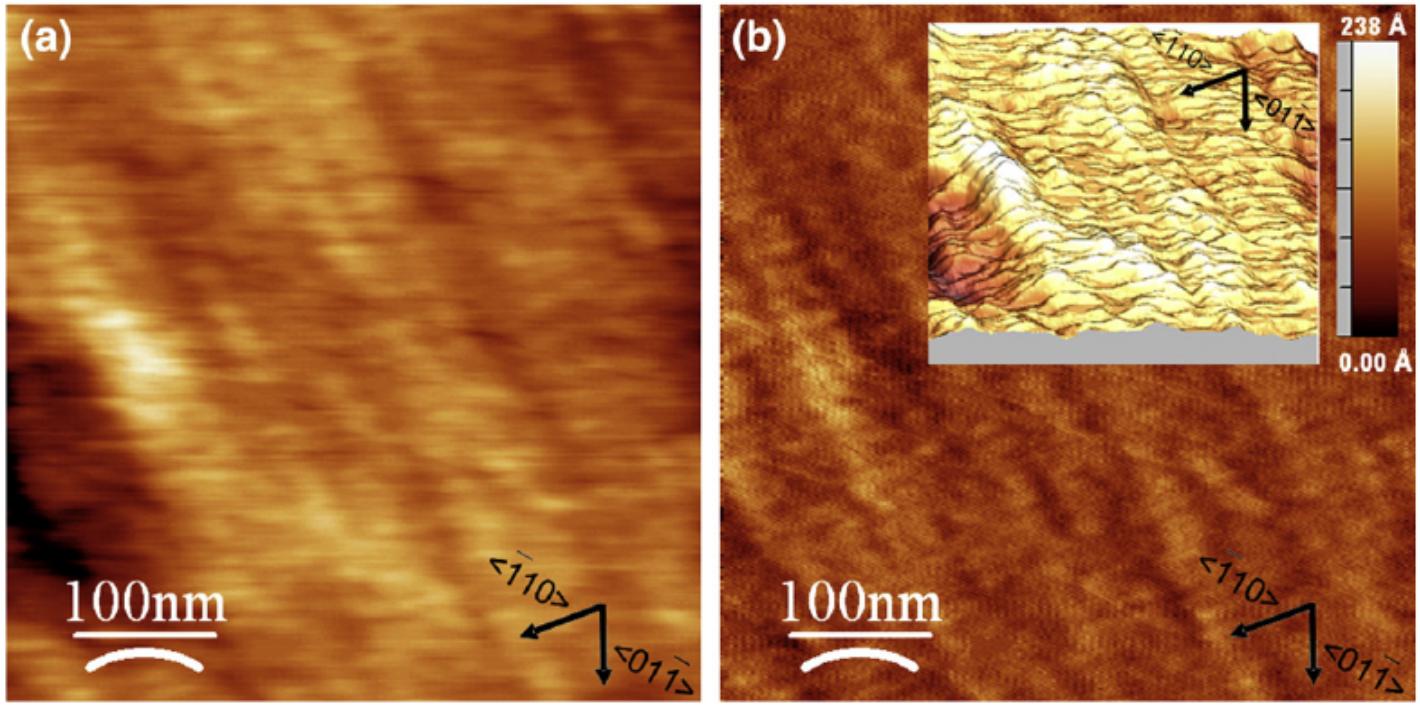

"Surface structure of magnetite (111) under hydrated conditions by crystal truncation rod diffraction," S.C. petitto et al. *Surf. Sci.* **604**, 1082-1093 (2010).

Magnetite (111) surface

Crystal truncation rod measurements require an oriented single crystal with a polished and cleaned surface.

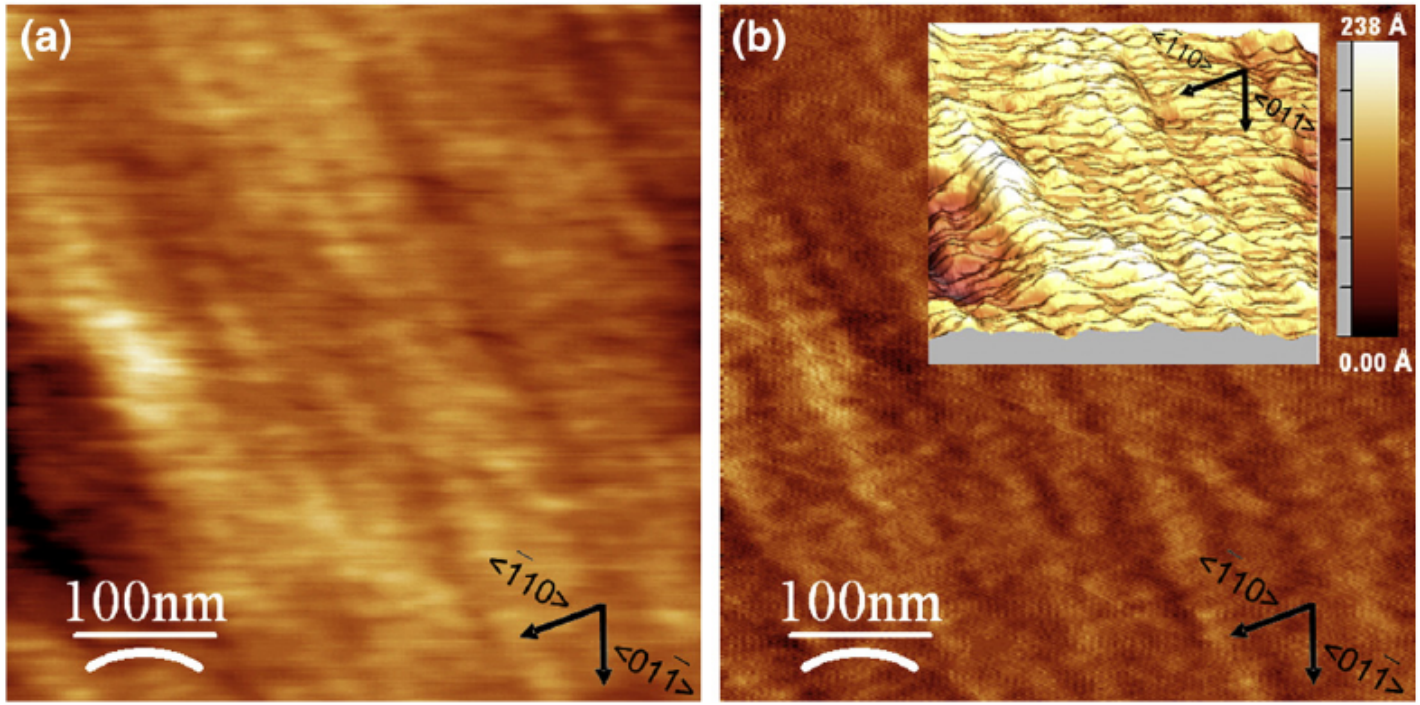

The final polished surface has clear terraces of between 150 Å–700 Å and a surface roughness of about 1.4 Å as seen in the inset from the atomic force microscopy images

"Surface structure of magnetite (111) under hydrated conditions by crystal truncation rod diffraction," S.C. petitto et al. *Surf. Sci.* **604**, 1082-1093 (2010).

CTR data and modeling

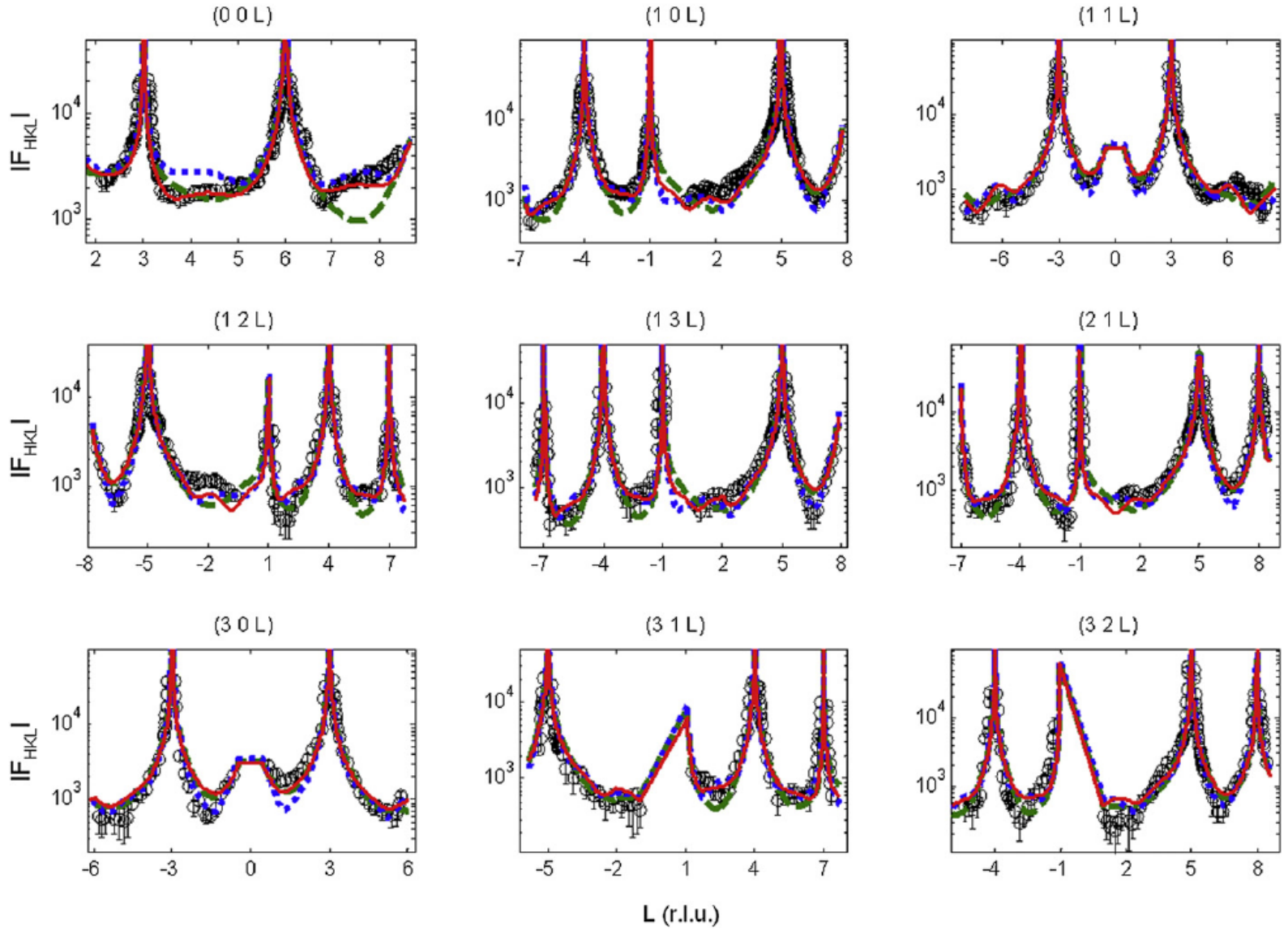

"Surface structure of magnetite (111) under hydrated conditions by crystal truncation rod diffraction," S.C. petitto et al. *Surf. Sci.* **604**, 1082-1093 (2010).

Hydrated surface of magnetite

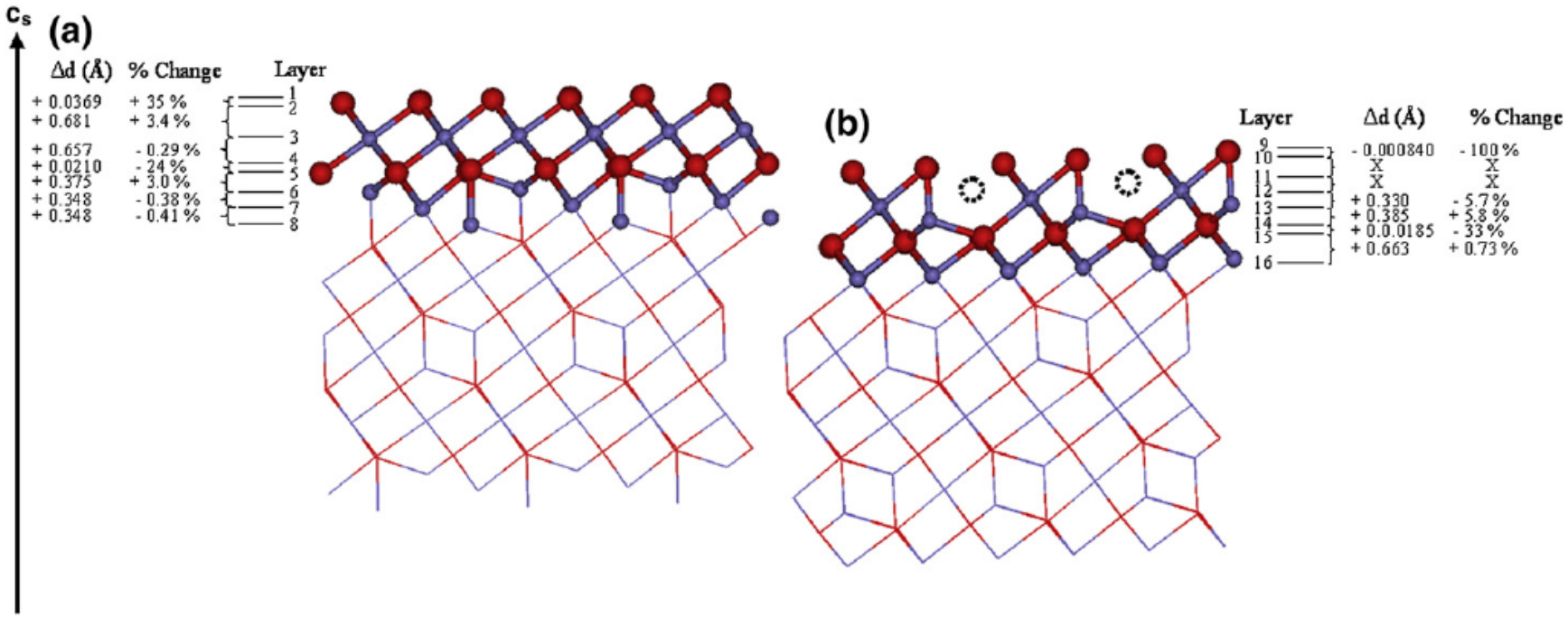

"Surface structure of magnetite (111) under hydrated conditions by crystal truncation rod diffraction," S.C. petitto et al. *Surf. Sci.* **604**, 1082-1093 (2010).

Hydrated surface of magnetite

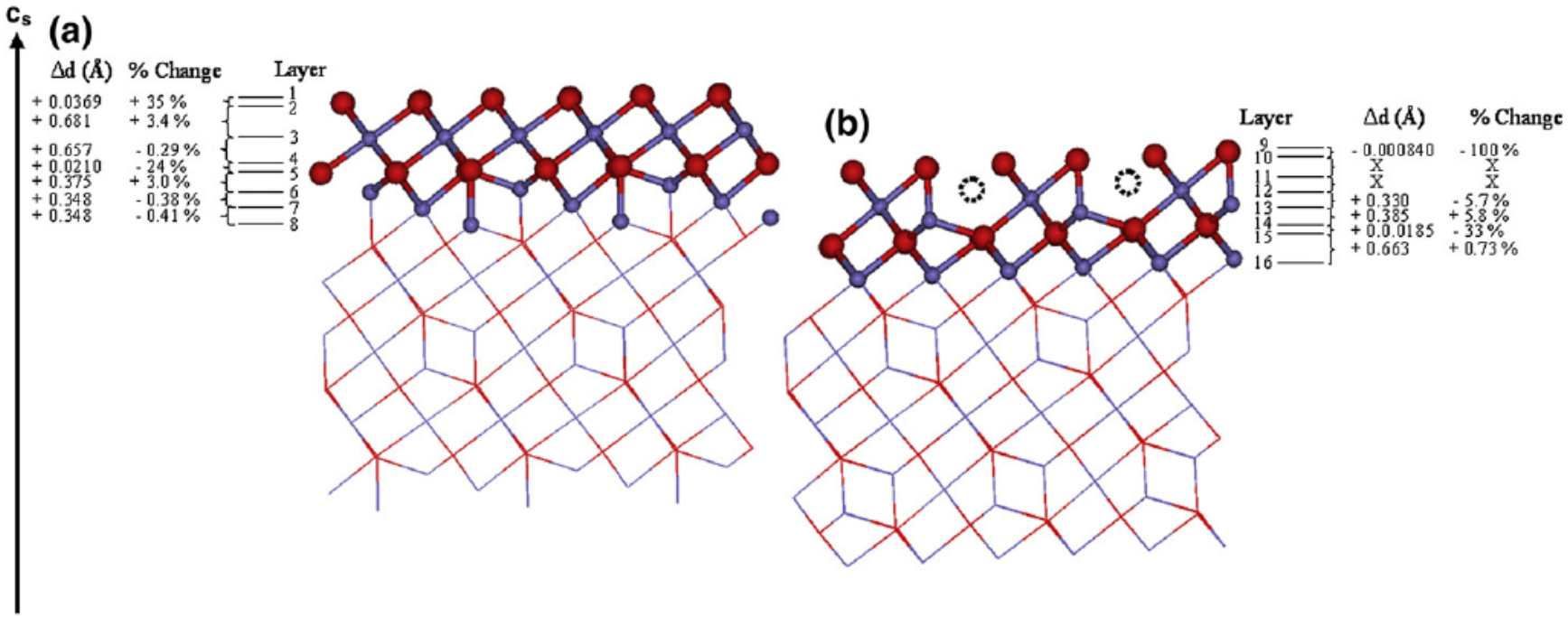

The result of the modeling of the CTR data indicates that the surface is 75% OOI and 25% OMI

"Surface structure of magnetite (111) under hydrated conditions by crystal truncation rod diffraction," S.C. petitto et al. *Surf. Sci.* **604**, 1082-1093 (2010).

Hydrated surface of magnetite

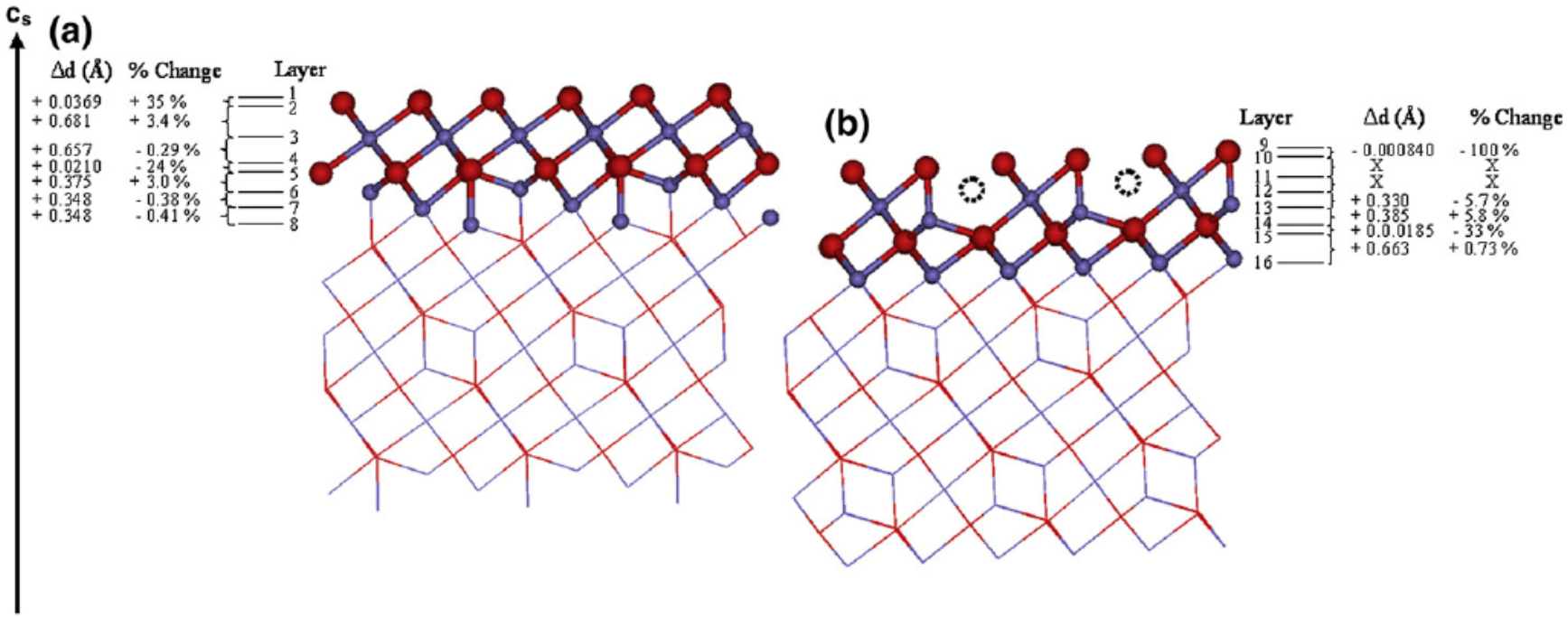

The result of the modeling of the CTR data indicates that the surface is 75% OOI and 25% OMI

The modeling also can provide details about the distance changes in the first layers at the surface

"Surface structure of magnetite (111) under hydrated conditions by crystal truncation rod diffraction," S.C. petitto et al. *Surf. Sci.* **604**, 1082-1093 (2010).

Buried interfaces of Ag films on silicon

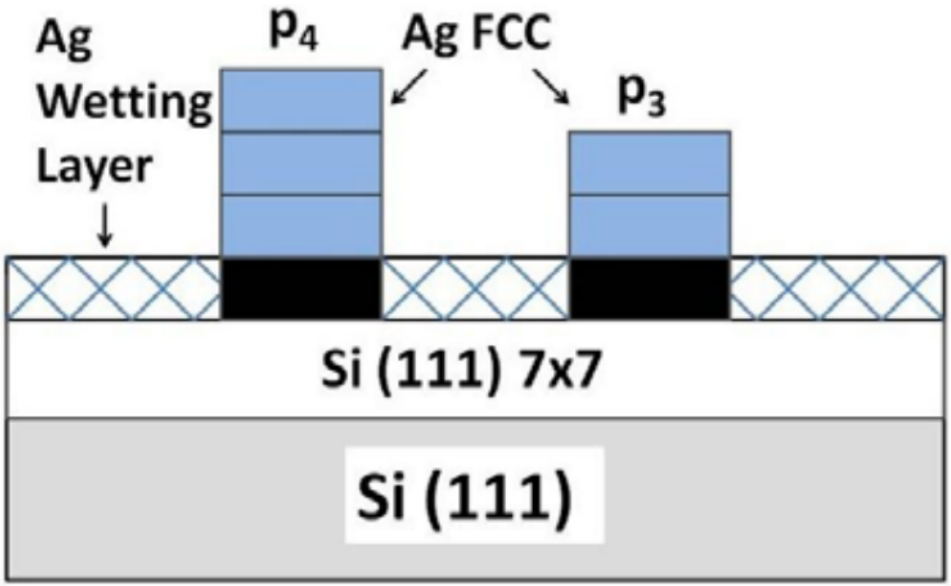

"Critical role of a buried interface in the Stranski-Krastanov growth of metallic nanocrystals: Quantum size effects in Ag/Si(111)-(7×7)," Y. Chen et al. *Phys. Rev. Lett.* **114**, 035501 (2015).

Buried interfaces of Ag films on silicon

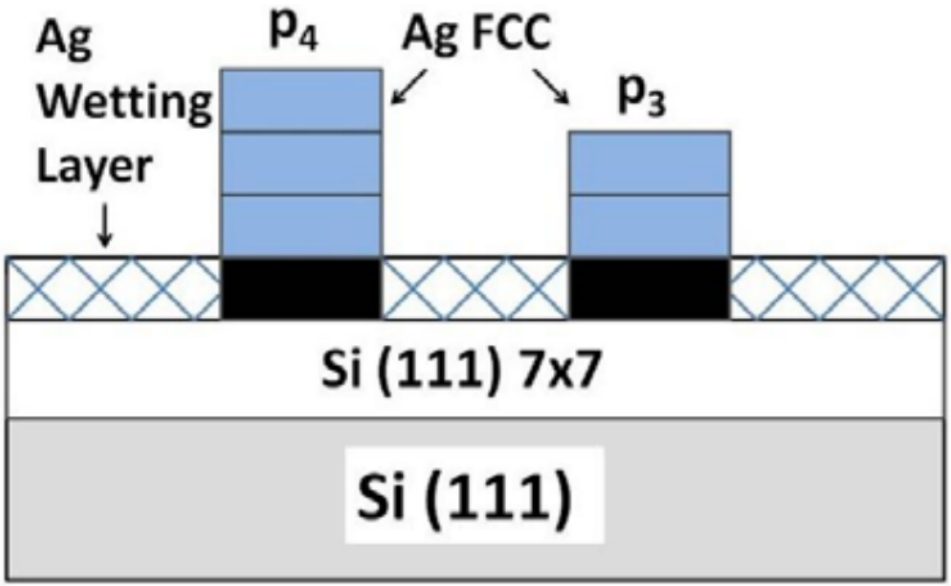

Understanding the process of surface wetting during thin film deposition is crucial to the semiconductor industry

"Critical role of a buried interface in the Stranski-Krastanov growth of metallic nanocrystals: Quantum size effects in Ag/Si(111)-(7×7)," Y. Chen et al. *Phys. Rev. Lett.* **114**, 035501 (2015).

Buried interfaces of Ag films on silicon

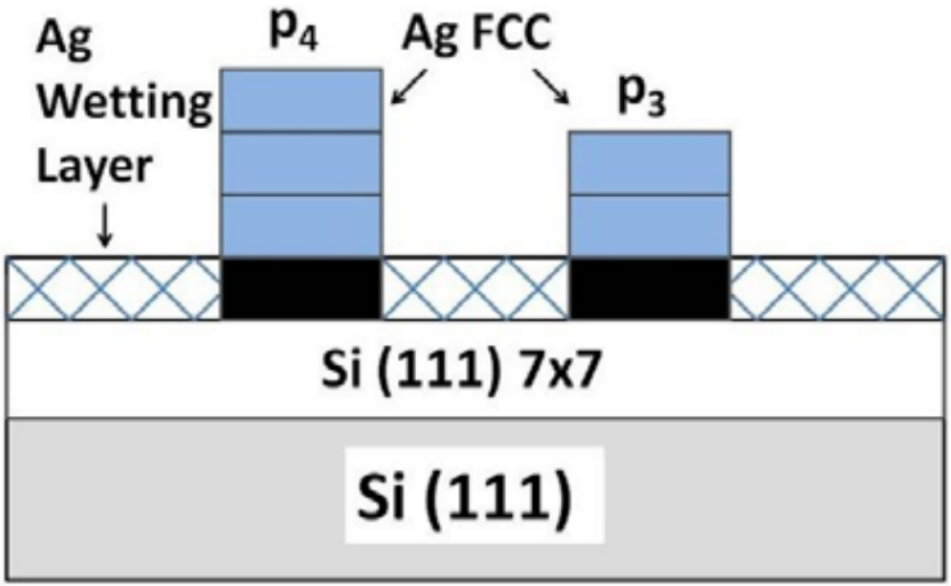

Understanding the process of surface wetting during thin film deposition is crucial to the semiconductor industry

This study uses at *in situ* reflectivity and CTR measurements to study the structural details of Ag film growth on a Si (111) surface

"Critical role of a buried interface in the Stranski-Krastanov growth of metallic nanocrystals: Quantum size effects in Ag/Si(111)-(7×7)," Y. Chen et al. *Phys. Rev. Lett.* **114**, 035501 (2015).

Buried interfaces of Ag films on silicon

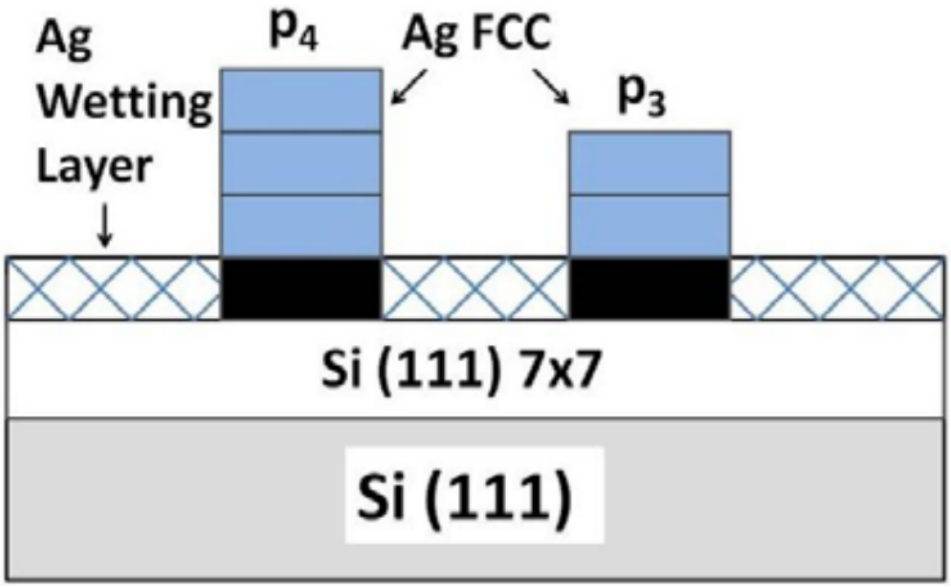

Understanding the process of surface wetting during thin film deposition is crucial to the semiconductor industry

This study uses at *in situ* reflectivity and CTR measurements to study the structural details of Ag film growth on a Si (111) surface

A Si(111) crystal is placed in an ultra-high vacuum chamber and flash-annealed to clean and reconstruct the surface

"Critical role of a buried interface in the Stranski-Krastanov growth of metallic nanocrystals: Quantum size effects in Ag/Si(111)-(7×7)," Y. Chen et al. *Phys. Rev. Lett.* **114**, 035501 (2015).

Buried interfaces of Ag films on silicon

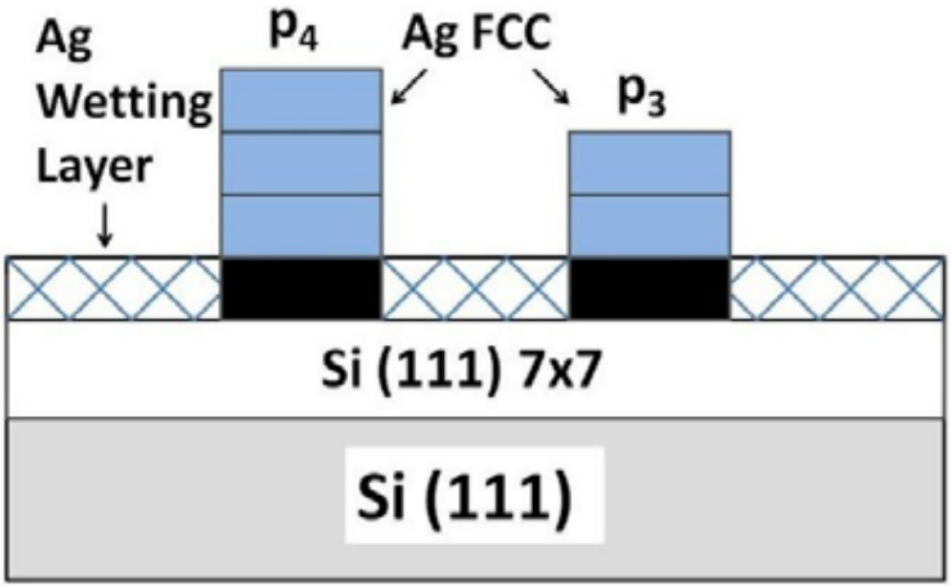

Understanding the process of surface wetting during thin film deposition is crucial to the semiconductor industry

This study uses at *in situ* reflectivity and CTR measurements to study the structural details of Ag film growth on a Si (111) surface

A Si(111) crystal is placed in an ultra-high vacuum chamber and flash-annealed to clean and reconstruct the surface

Ag was thermally evaporated on the surface and both reflectivity measurements of the surface and CTR measurements of the Ag (001) growth layer were performed

"Critical role of a buried interface in the Stranski-Krastanov growth of metallic nanocrystals: Quantum size effects in Ag/Si(111)-(7×7)," Y. Chen et al. *Phys. Rev. Lett.* **114**, 035501 (2015).

Reflectivity & CTR measurements

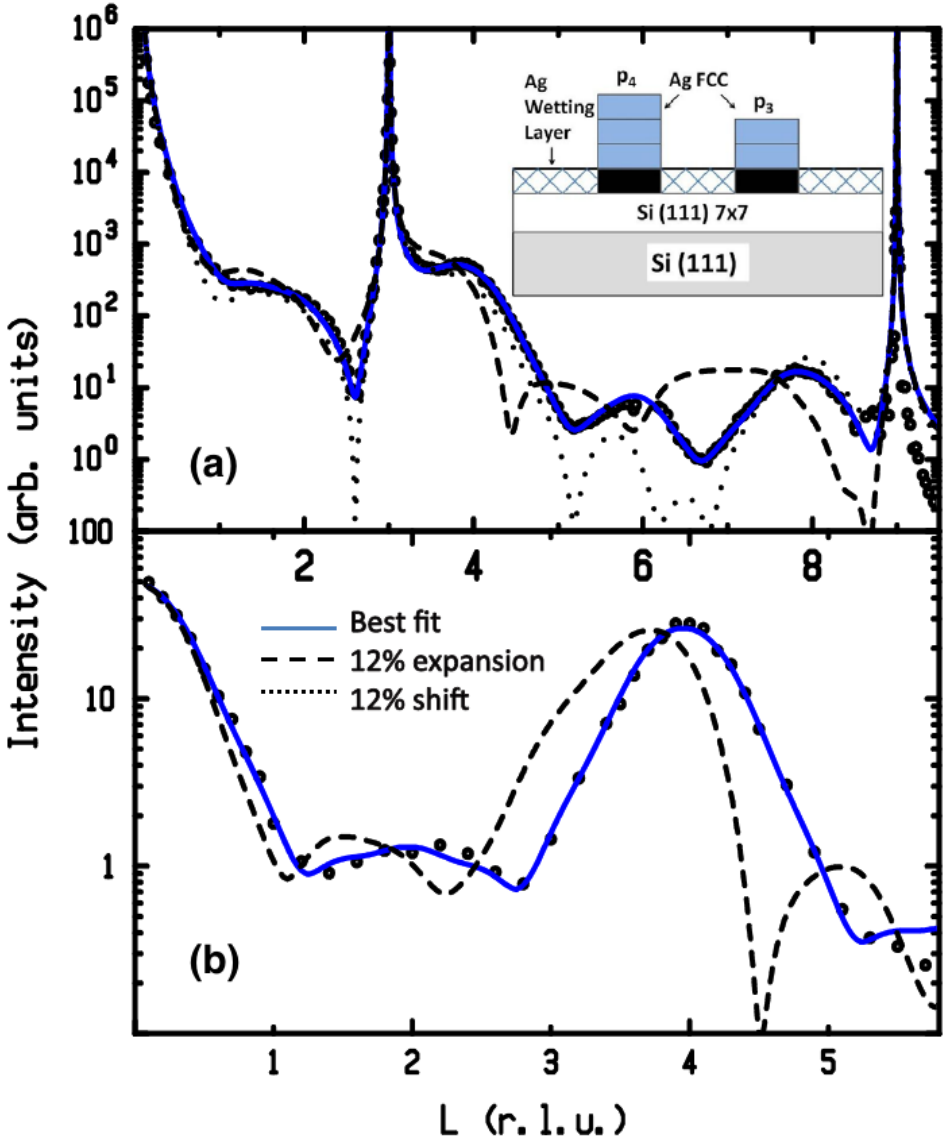

"Critical role of a buried interface in the Stranski-Krastanov growth of metallic nanocrystals: Quantum size effects in Ag/Si(111)-(7×7)," Y. Chen et al. *Phys. Rev. Lett.* **114**, 035501 (2015).

Reflectivity & CTR measurements

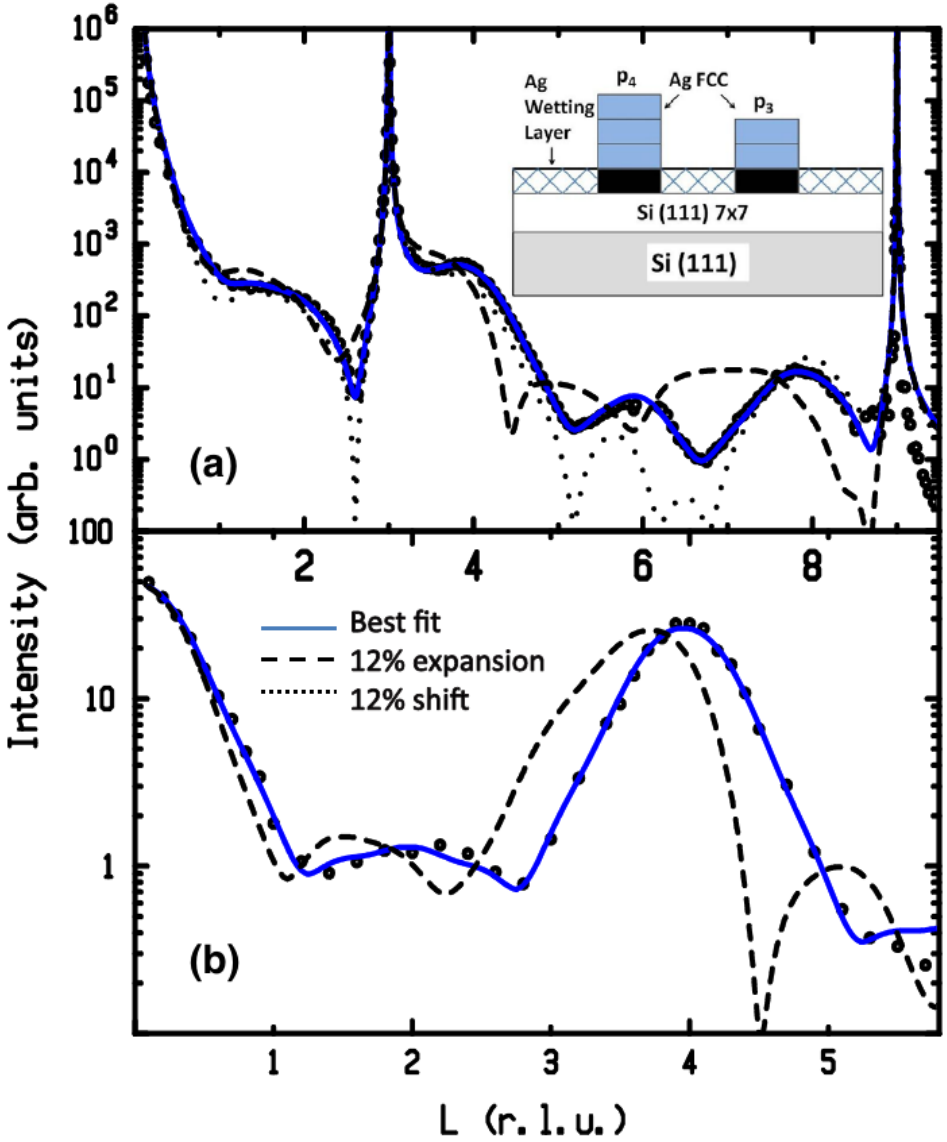

Reflectivity "sees" the entire surface while CTR measures only the incommensurate Ag crystalline layer on the surface

"Critical role of a buried interface in the Stranski-Krastanov growth of metallic nanocrystals: Quantum size effects in Ag/Si(111)-(7×7)," Y. Chen et al. *Phys. Rev. Lett.* **114**, 035501 (2015).

Reflectivity & CTR measurements

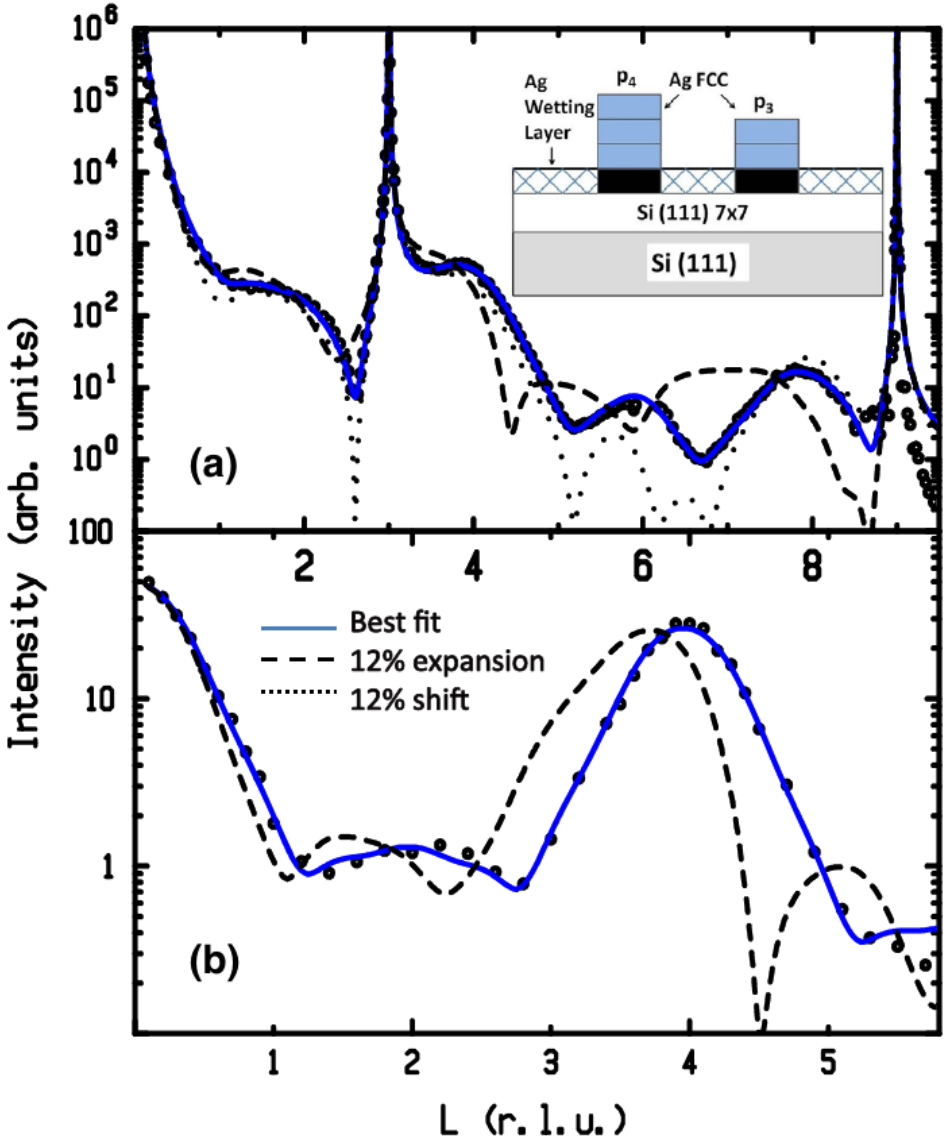

Reflectivity "sees" the entire surface while CTR measures only the incommensurate Ag crystalline layer on the surface

At 0.9 monolayer of Ag the reflectivity shows 3 layers as does the CTR measurement

"Critical role of a buried interface in the Stranski-Krastanov growth of metallic nanocrystals: Quantum size effects in Ag/Si(111)-(7×7)," Y. Chen et al. *Phys. Rev. Lett.* **114**, 035501 (2015).

Reflectivity & CTR measurements

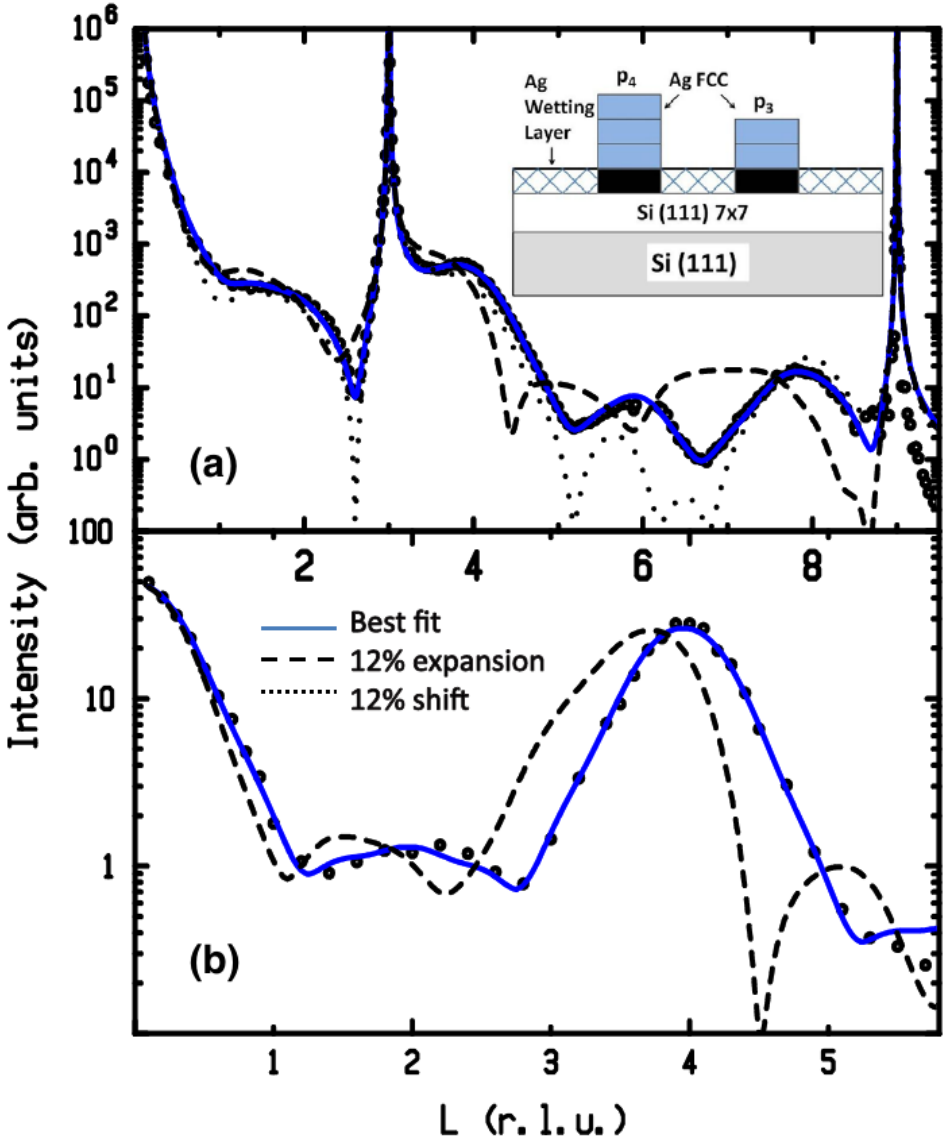

Reflectivity "sees" the entire surface while CTR measures only the incommensurate Ag crystalline layer on the surface

At 0.9 monolayer of Ag the reflectivity shows 3 layers as does the CTR measurement

These results indicate that the islands have an incommensurate Ag fcc structure all the way to the surface while the wetting layer is commensurate with the Si (111)

"Critical role of a buried interface in the Stranski-Krastanov growth of metallic nanocrystals: Quantum size effects in Ag/Si(111)-(7×7)," Y. Chen et al. *Phys. Rev. Lett.* **114**, 035501 (2015).

Reflectivity & CTR measurements

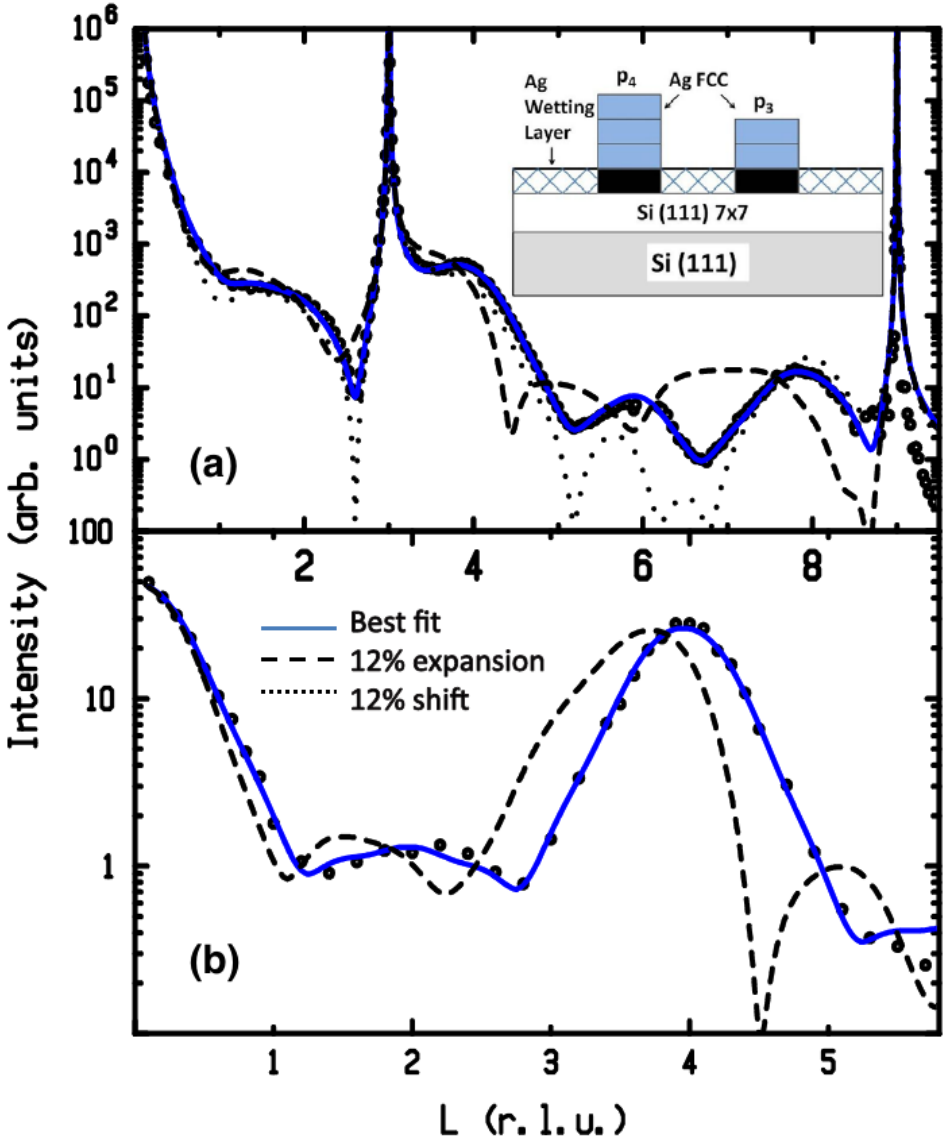

Reflectivity "sees" the entire surface while CTR measures only the incommensurate Ag crystalline layer on the surface

At 0.9 monolayer of Ag the reflectivity shows 3 layers as does the CTR measurement

These results indicate that the islands have an incommensurate Ag fcc structure all the way to the surface while the wetting layer is commensurate with the Si (111)

Modeling shows that the islands are displaced from the surface

"Critical role of a buried interface in the Stranski-Krastanov growth of metallic nanocrystals: Quantum size effects in Ag/Si(111)-(7×7)," Y. Chen et al. *Phys. Rev. Lett.* **114**, 035501 (2015).

Ag island height & quantum confinement

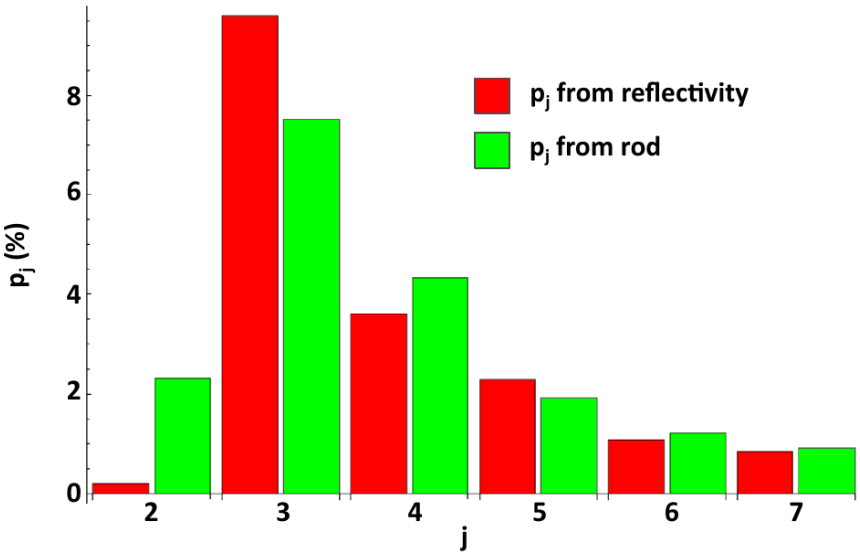

"Critical role of a buried interface in the Stranski-Krastanov growth of metallic nanocrystals: Quantum size effects in Ag/Si(111)-(7×7)," Y. Chen et al. *Phys. Rev. Lett.* **114**, 035501 (2015).

Ag island height & quantum confinement

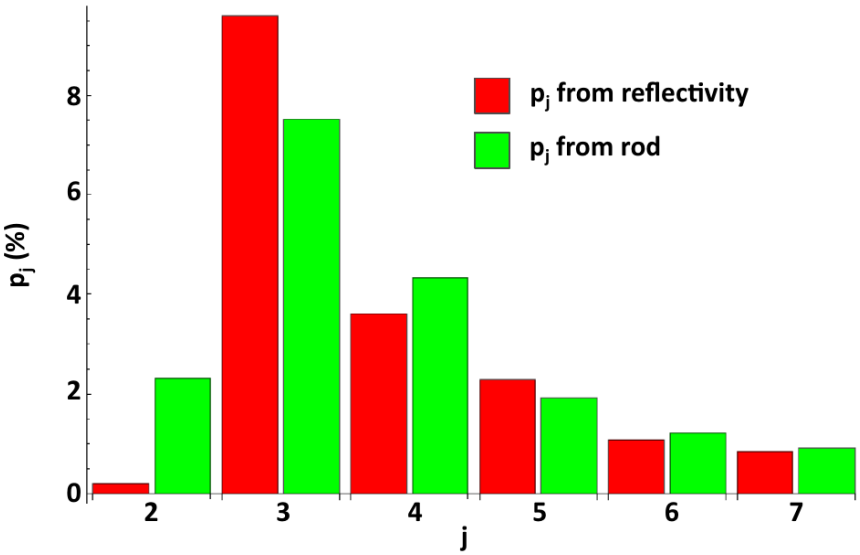

Island layer height distributions from reflectivity and CTR are well correlated and indicate that 3 layers are the minimum for stability

"Critical role of a buried interface in the Stranski-Krastanov growth of metallic nanocrystals: Quantum size effects in Ag/Si(111)-(7×7)," Y. Chen et al. *Phys. Rev. Lett.* **114**, 035501 (2015).

Ag island height & quantum confinement

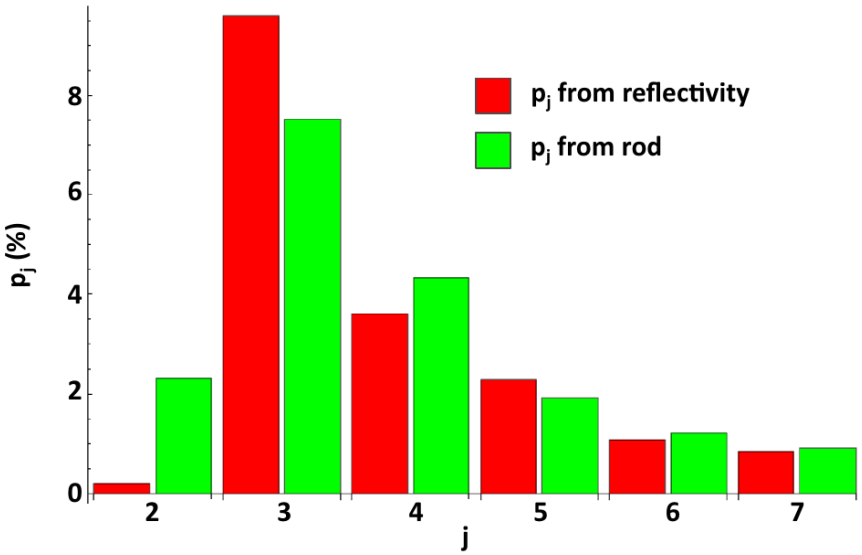

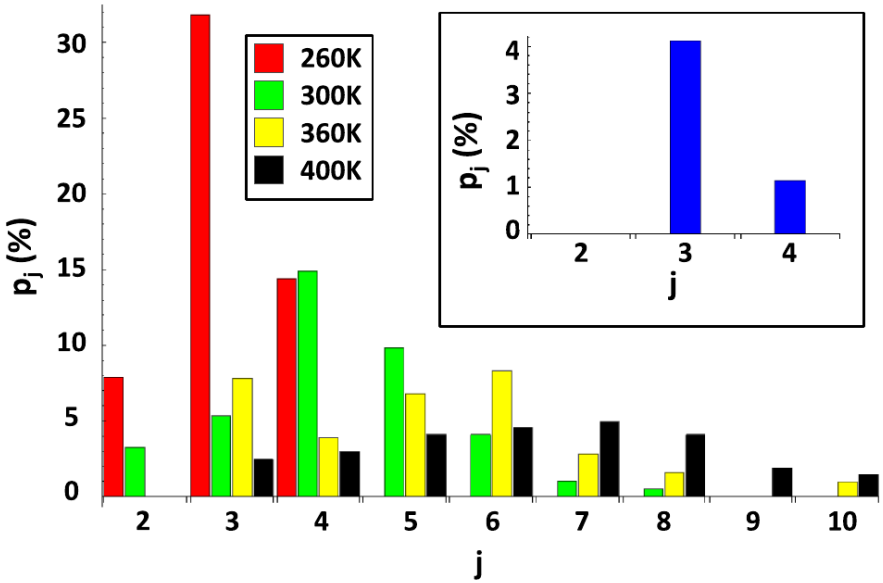

Island layer height distributions from reflectivity and CTR are well correlated and indicate that 3 layers are the minimum for stability

"Critical role of a buried interface in the Stranski-Krastanov growth of metallic nanocrystals: Quantum size effects in Ag/Si(111)-(7×7)," Y. Chen et al. *Phys. Rev. Lett.* **114**, 035501 (2015).

Ag island height & quantum confinement

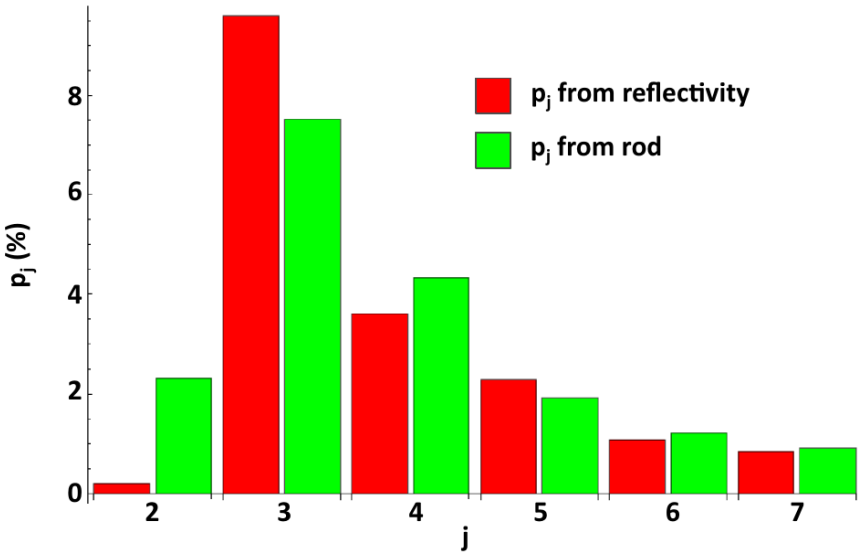

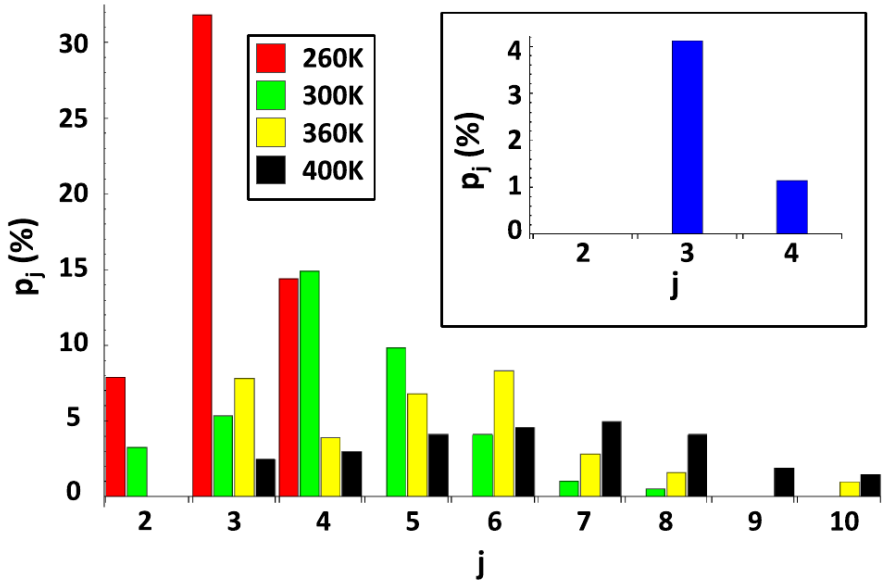

Island layer height distributions from reflectivity and CTR are well correlated and indicate that 3 layers are the minimum for stability

Depositions as a function of temperature show that the island height distribution increases and broadens due to mobility of Ag atoms

"Critical role of a buried interface in the Stranski-Krastanov growth of metallic nanocrystals: Quantum size effects in Ag/Si(111)-(7×7)," Y. Chen et al. *Phys. Rev. Lett.* **114**, 035501 (2015).

Ag island height & quantum confinement

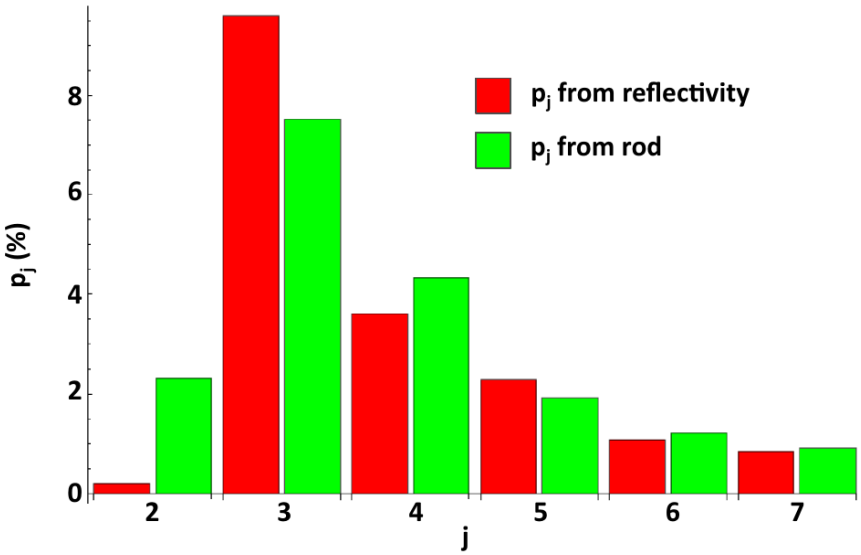

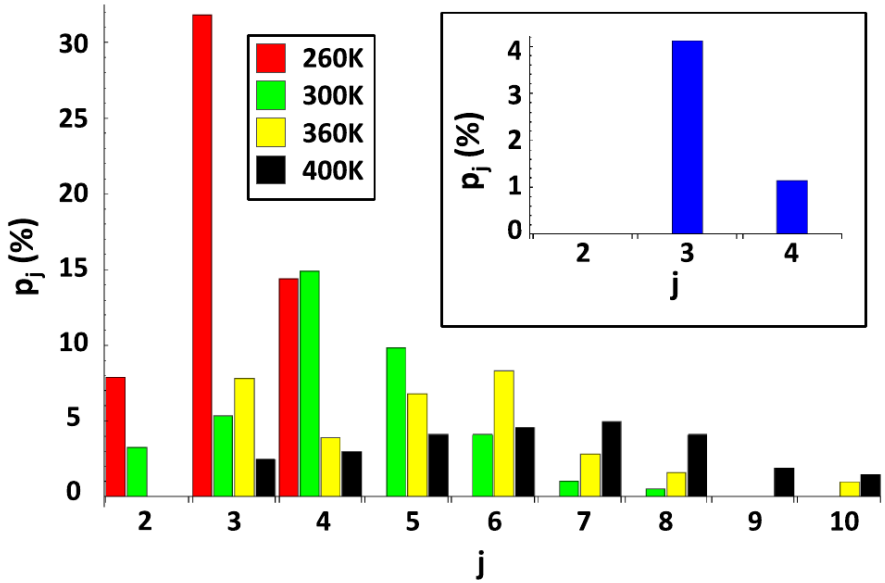

Island layer height distributions from reflectivity and CTR are well correlated and indicate that 3 layers are the minimum for stability

Depositions as a function of temperature show that the island height distribution increases and broadens due to mobility of Ag atoms

The exceptional stability of the three layer islands is consistent with quantum confinement effects that drive the growth process

"Critical role of a buried interface in the Stranski-Krastanov growth of metallic nanocrystals: Quantum size effects in Ag/Si(111)-(7×7)," Y. Chen et al. *Phys. Rev. Lett.* **114**, 035501 (2015).

In plane structure of islands

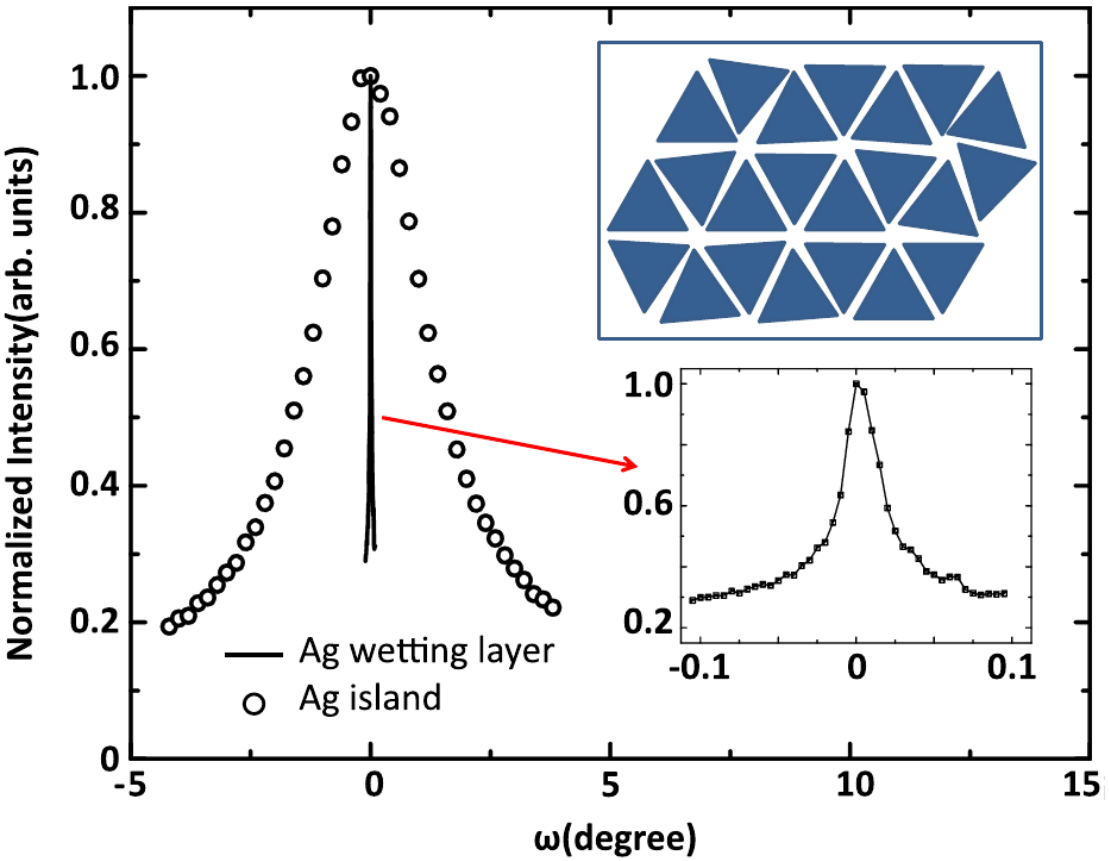

"Critical role of a buried interface in the Stranski-Krastanov growth of metallic nanocrystals: Quantum size effects in Ag/Si(111)-(7×7)," Y. Chen et al. *Phys. Rev. Lett.* **114**, 035501 (2015).

In plane structure of islands

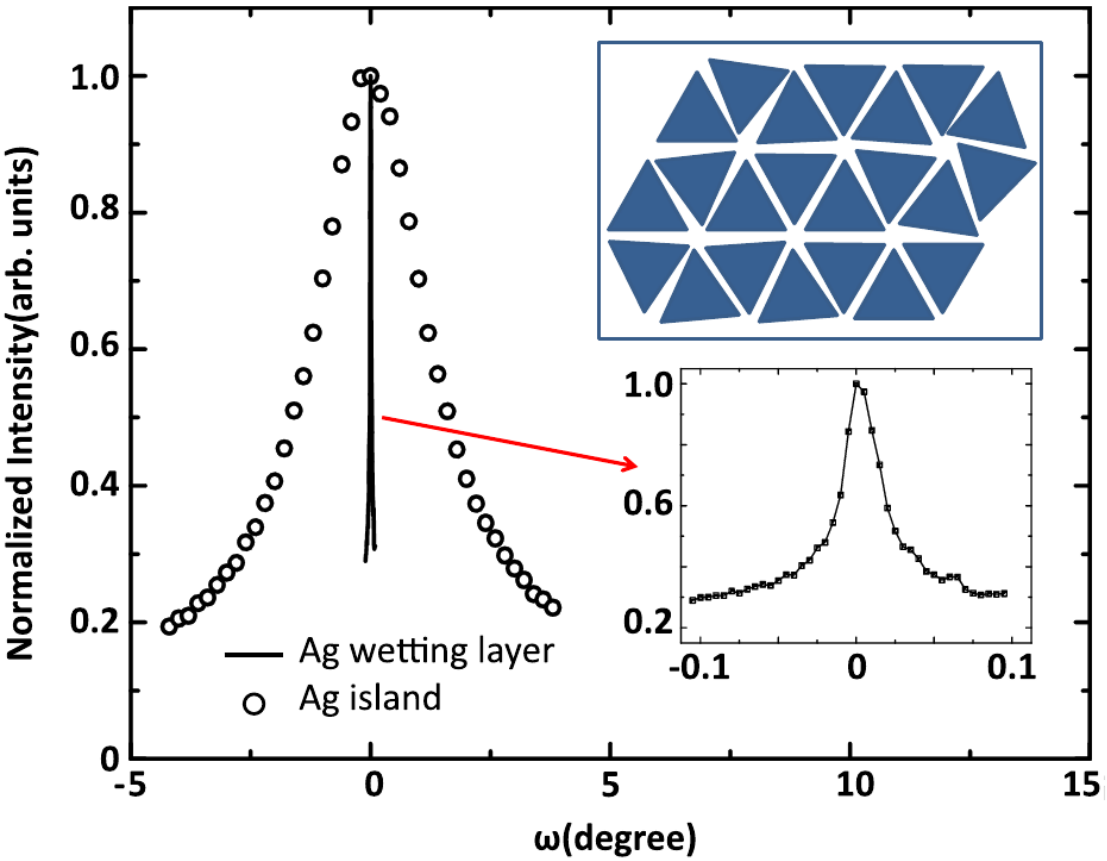

The large in-plane orientational disorder can be seen from the azimuthal scattering profile that is 3 degrees wide

"Critical role of a buried interface in the Stranski-Krastanov growth of metallic nanocrystals: Quantum size effects in Ag/Si(111)-(7×7)," Y. Chen et al. *Phys. Rev. Lett.* **114**, 035501 (2015).

In plane structure of islands

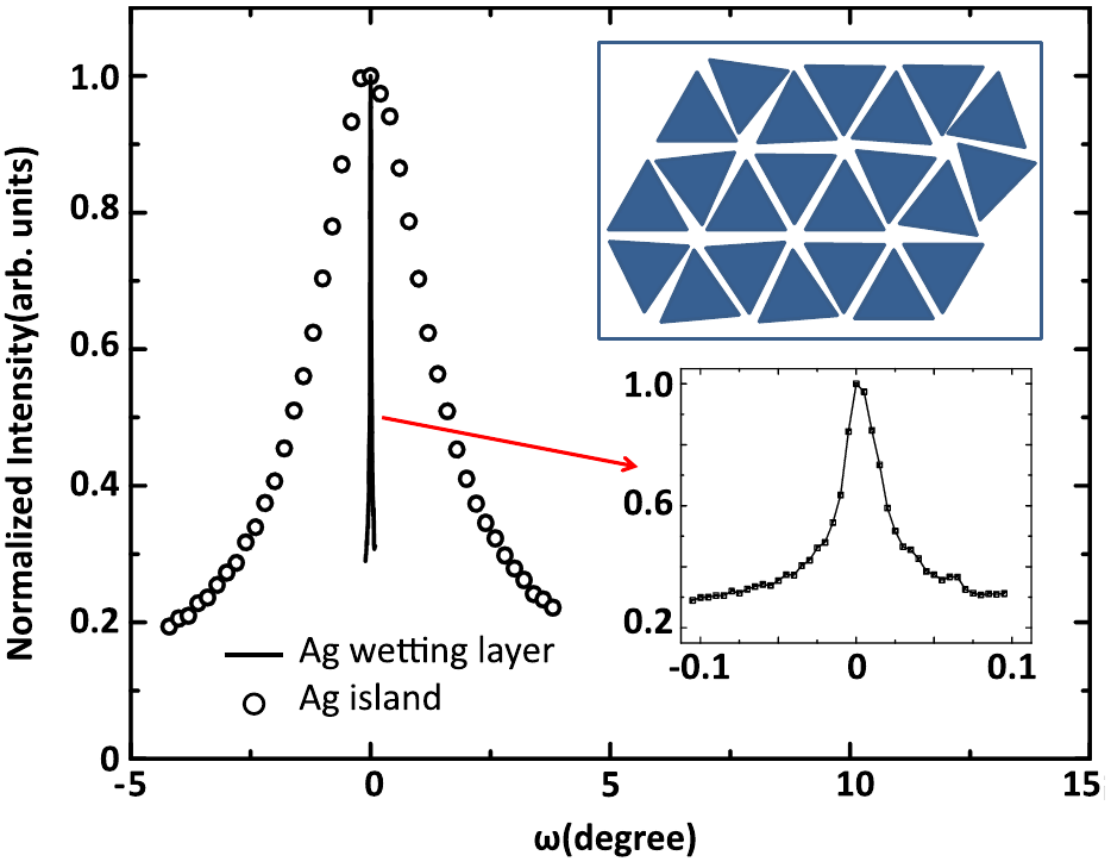

The large in-plane orientational disorder can be seen from the azimuthal scattering profile that is 3 degrees wide The narrow peak is the azimuthal scan of the commensurate wetting layer

"Critical role of a buried interface in the Stranski-Krastanov growth of metallic nanocrystals: Quantum size effects in Ag/Si(111)-(7×7)," Y. Chen et al. *Phys. Rev. Lett.* **114**, 035501 (2015).

In plane structure of islands

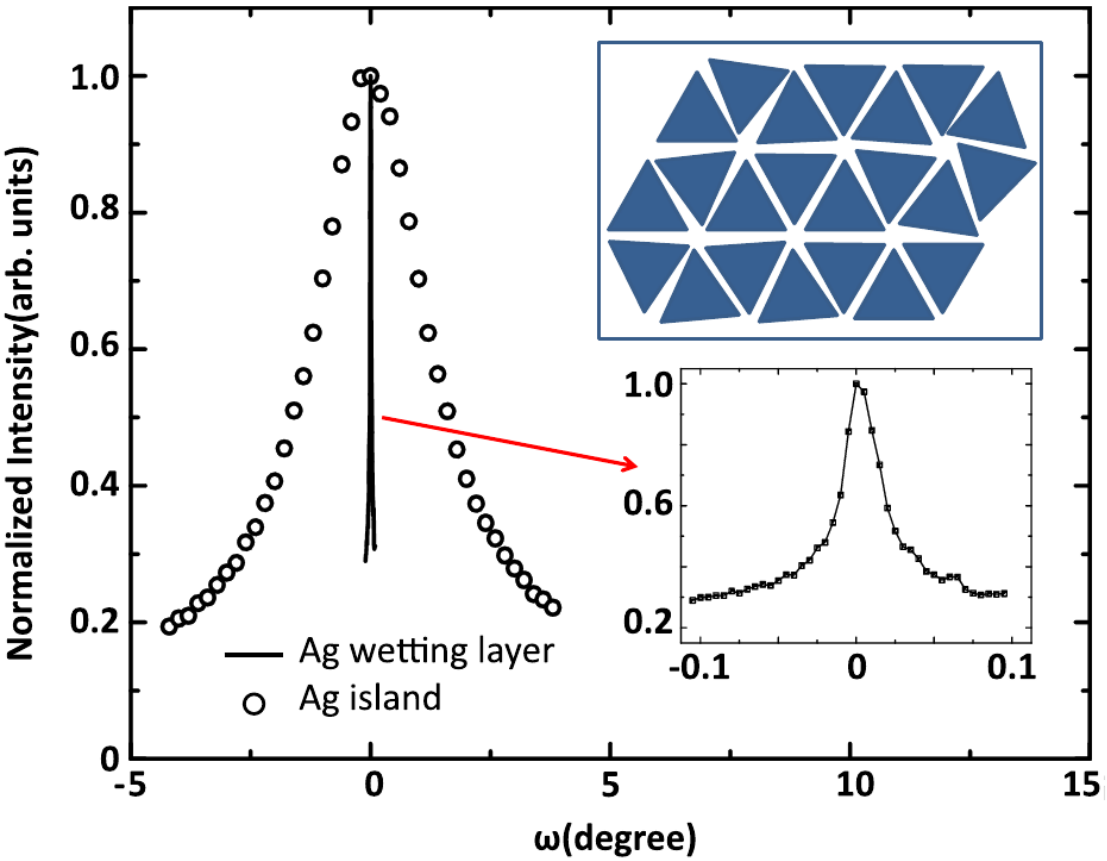

The large in-plane orientational disorder can be seen from the azimuthal scattering profile that is 3 degrees wide The narrow peak is the azimuthal scan of the commensurate wetting layer

The islands thus have a weak interaction with the substrate compared to the wetting layer

"Critical role of a buried interface in the Stranski-Krastanov growth of metallic nanocrystals: Quantum size effects in Ag/Si(111)-(7×7)," Y. Chen et al. *Phys. Rev. Lett.* **114**, 035501 (2015).

Modulated structures

By definition crystals have always been considered to have long range order.

Modulated structures

By definition crystals have always been considered to have long range order.

However, it is common to see structures where the positions of the atoms is modulated (e.g. charge density waves, magnetic lattices, etc.) according to $x_n = an + u\cos(qan)$, where: a is the lattice parameter, u is the amplitude of the displacement, and $q = 2\pi/\lambda_m$ is the wave vector of the modulation.

Modulated structures

By definition crystals have always been considered to have long range order.

However, it is common to see structures where the positions of the atoms is modulated (e.g. charge density waves, magnetic lattices, etc.) according to $x_n = an + u\cos(qan)$, where: a is the lattice parameter, u is the amplitude of the displacement, and $q = 2\pi/\lambda_m$ is the wave vector of the modulation.

If λ_m is a multiple or a rational fraction of a, it is called a commensurate modulation

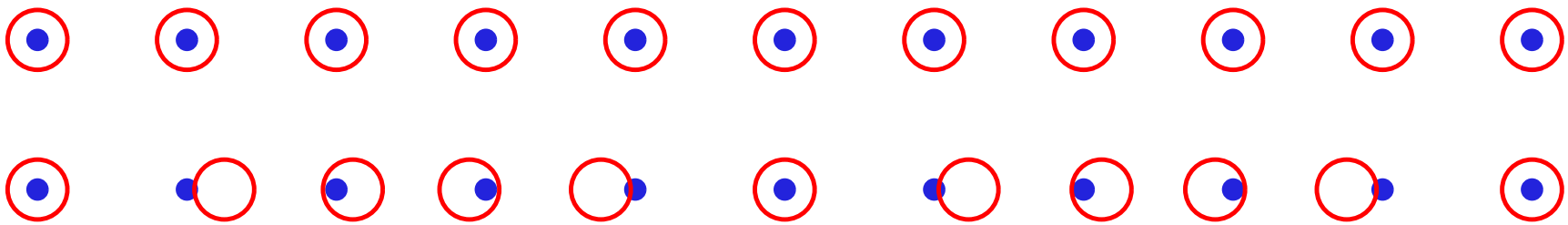

Modulated structures

By definition crystals have always been considered to have long range order.

However, it is common to see structures where the positions of the atoms is modulated (e.g. charge density waves, magnetic lattices, etc.) according to $x_n = an + u\cos(qan)$, where: a is the lattice parameter, u is the amplitude of the displacement, and $q = 2\pi/\lambda_m$ is the wave vector of the modulation.

If λ_m is a multiple or a rational fraction of a, it is called a commensurate modulation but if $\lambda_m = ca$, where c is an irrational number, then it is an incommensurate modulation.

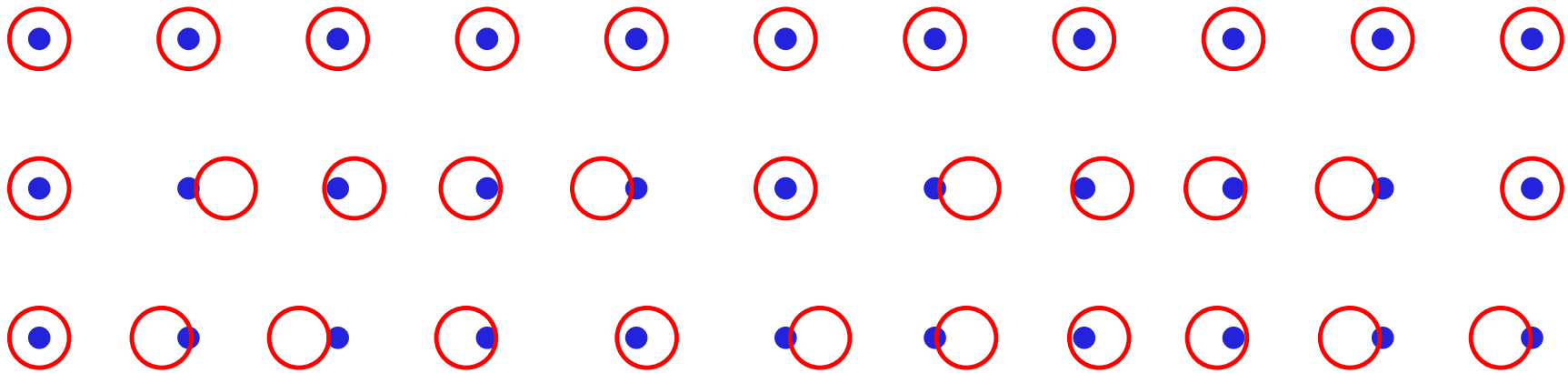

Diffraction from a modulation

For simple a 1D modulated structure, we can compute the scattering

Diffraction from a modulation

For simple a 1D modulated structure, we can compute the scattering

$$A(Q) = \sum_{n=0}^{N-1} e^{iQx_n}$$

Diffraction from a modulation

For simple a 1D modulated structure, we can compute the scattering assuming

$$x_n = an + u\cos(qan)$$

and that the scattering factor for each atom is set to unity

$$A(Q) = \sum_{n=0}^{N-1} e^{iQx_n}$$

Diffraction from a modulation

For simple a 1D modulated structure, we can compute the scattering assuming

$$x_n = an + u\cos(qan)$$

and that the scattering factor for each atom is set to unity

$$A(Q) = \sum_{n=0}^{N-1} e^{iQx_n} = \sum_{n=0}^{N-1} e^{iQ[an+u\cos(qan)]}$$

Diffraction from a modulation

For simple a 1D modulated structure, we can compute the scattering assuming

$$x_n = an + u\cos(qan)$$

and that the scattering factor for each atom is set to unity

$$A(Q) = \sum_{n=0}^{N-1} e^{iQx_n} = \sum_{n=0}^{N-1} e^{iQ[an+u\cos(qan)]}$$
$$= \sum_{n=0}^{N-1} e^{iQan}\, e^{iQu\cos(qan)}$$

Diffraction from a modulation

For simple a 1D modulated structure, we can compute the scattering assuming

$$x_n = an + u\cos(qan)$$

and that the scattering factor for each atom is set to unity

for the displacement u small, this becomes

$$A(Q) = \sum_{n=0}^{N-1} e^{iQx_n} = \sum_{n=0}^{N-1} e^{iQ[an+u\cos(qan)]}$$
$$= \sum_{n=0}^{N-1} e^{iQan} e^{iQu\cos(qan)}$$

Diffraction from a modulation

For simple a 1D modulated structure, we can compute the scattering assuming

$$x_n = an + u\cos(qan)$$

and that the scattering factor for each atom is set to unity

for the displacement u small, this becomes

$$A(Q) = \sum_{n=0}^{N-1} e^{iQx_n} = \sum_{n=0}^{N-1} e^{iQ[an+u\cos(qan)]}$$

$$= \sum_{n=0}^{N-1} e^{iQan} e^{iQu\cos(qan)}$$

$$A(Q) \approx \sum_{n=0}^{N-1} e^{iQan} [1 + iQu\cos(qan) + \cdots]$$

Diffraction from a modulation

For simple a 1D modulated structure, we can compute the scattering assuming

$$x_n = an + u\cos(qan)$$

and that the scattering factor for each atom is set to unity

$$A(Q) = \sum_{n=0}^{N-1} e^{iQx_n} = \sum_{n=0}^{N-1} e^{iQ[an+u\cos(qan)]}$$
$$= \sum_{n=0}^{N-1} e^{iQan} e^{iQu\cos(qan)}$$

for the displacement u small, this becomes

$$A(Q) \approx \sum_{n=0}^{N-1} e^{iQan} [1 + iQu\cos(qan) + \cdots]$$

$$A(Q) \approx \sum_{n=0}^{N-1} e^{iQan} + i\left(\frac{Qu}{2}\right)\left[e^{i(Q+q)an} + e^{-i(Q-q)an}\right]$$

Diffraction from a modulation

For simple a 1D modulated structure, we can compute the scattering assuming

$$x_n = an + u\cos(qan)$$

and that the scattering factor for each atom is set to unity

$$A(Q) = \sum_{n=0}^{N-1} e^{iQx_n} = \sum_{n=0}^{N-1} e^{iQ[an+u\cos(qan)]}$$

$$= \sum_{n=0}^{N-1} e^{iQan}\, e^{iQu\cos(qan)}$$

for the displacement u small, this becomes

$$A(Q) \approx \sum_{n=0}^{N-1} e^{iQan}\left[1 + iQu\cos(qan) + \cdots\right]$$

$$A(Q) \approx \sum_{n=0}^{N-1} e^{iQan} + i\left(\frac{Qu}{2}\right)\left[e^{i(Q+q)an} + e^{-i(Q-q)an}\right]$$

$$I(Q) = N\left(\frac{2\pi}{a}\right)\sum_h \delta(Q-G_h) + \left(\frac{Qu}{2}\right)^2\left[\delta(Q+q-G_h) + \delta(Q-q-G_h)\right]$$

Diffraction from a modulation

For simple a 1D modulated structure, we can compute the scattering assuming

$$x_n = an + u\cos(qan)$$

and that the scattering factor for each atom is set to unity

$$A(Q) = \sum_{n=0}^{N-1} e^{iQx_n} = \sum_{n=0}^{N-1} e^{iQ[an+u\cos(qan)]}$$

$$= \sum_{n=0}^{N-1} e^{iQan}\, e^{iQu\cos(qan)}$$

for the displacement u small, this becomes

$$A(Q) \approx \sum_{n=0}^{N-1} e^{iQan}\left[1 + iQu\cos(qan) + \cdots\right]$$

$$A(Q) \approx \sum_{n=0}^{N-1} e^{iQan} + i\left(\frac{Qu}{2}\right)\left[e^{i(Q+q)an} + e^{-i(Q-q)an}\right]$$

$$I(Q) = N\left(\frac{2\pi}{a}\right)\sum_h \delta(Q-G_h) + \left(\frac{Qu}{2}\right)^2\left[\delta(Q+q-G_h) + \delta(Q-q-G_h)\right]$$

the diffraction pattern has main Bragg peaks plus satellite peaks

Quasiperiodic scattering

$$I(Q) = N\left(\frac{2\pi}{a}\right)\sum_h \delta(Q - G_h) + \left(\frac{Qu}{2}\right)^2\left[\delta(Q + q - G_h) + \delta(Q - q - G_h)\right]$$

Quasiperiodic scattering

$$I(Q) = N\left(\frac{2\pi}{a}\right)\sum_h \delta(Q-G_h) + \left(\frac{Qu}{2}\right)^2\left[\delta(Q+q-G_h) + \delta(Q-q-G_h)\right]$$

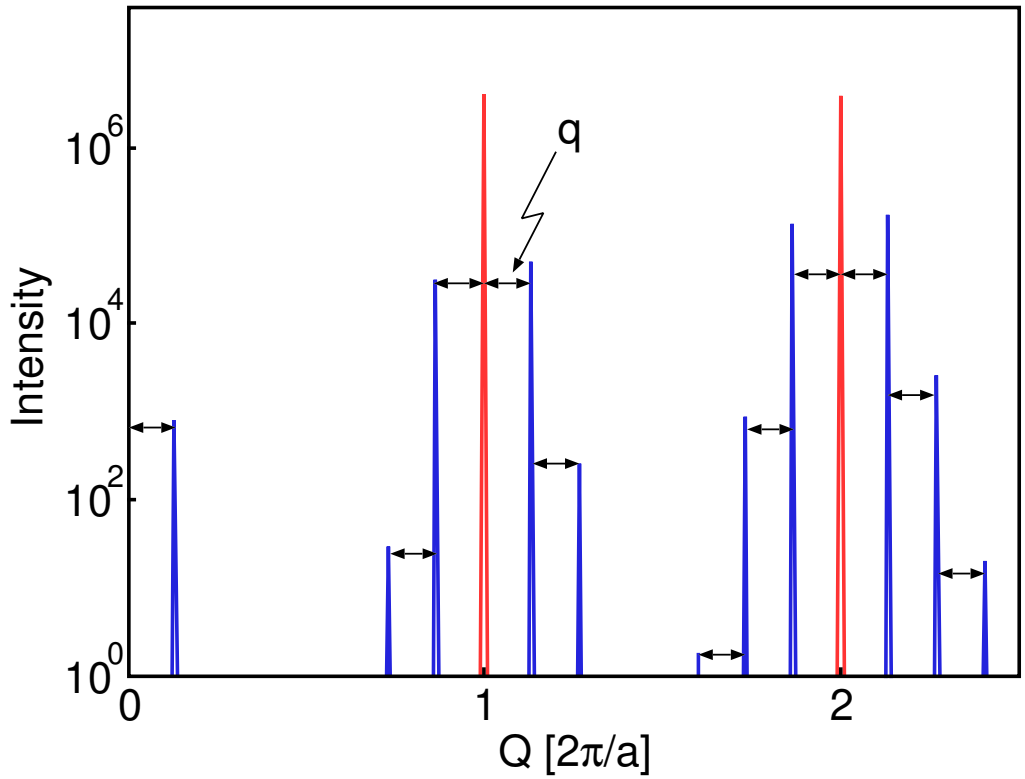

Quasiperiodic scattering

$$I(Q) = N\left(\frac{2\pi}{a}\right)\sum_h \delta(Q-G_h) + \left(\frac{Qu}{2}\right)^2\left[\delta(Q+q-G_h) + \delta(Q-q-G_h)\right]$$

This kind of scattering pattern holds for both commensurate and incommensurate modulations and there are multiple satellites around the $Q = 0$ as well as every main peak

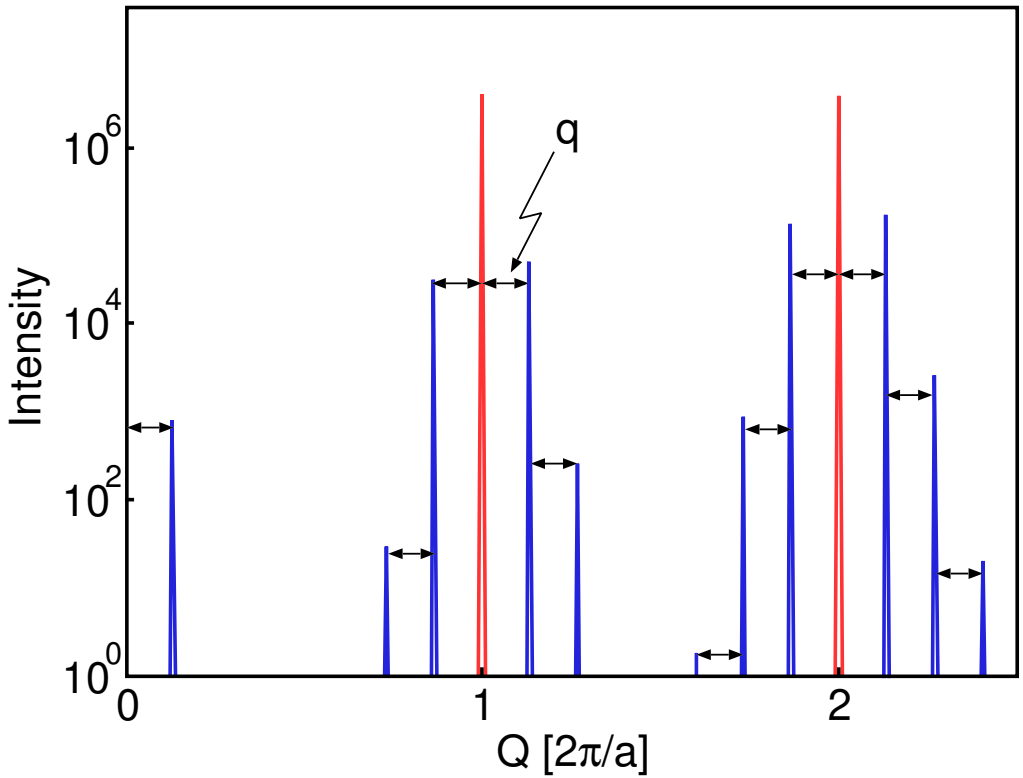

Quasiperiodic scattering

$$I(Q) = N\left(\frac{2\pi}{a}\right)\sum_h \delta(Q-G_h) + \left(\frac{Qu}{2}\right)^2\left[\delta(Q+q-G_h) + \delta(Q-q-G_h)\right]$$

This kind of scattering pattern holds for both commensurate and incommensurate modulations and there are multiple satellites around the $Q = 0$ as well as every main peak

If the modulation of the structure is a multiple of the lattice parameter, the modulation is simply a superlattice and the actual lattice parameter will be changed.

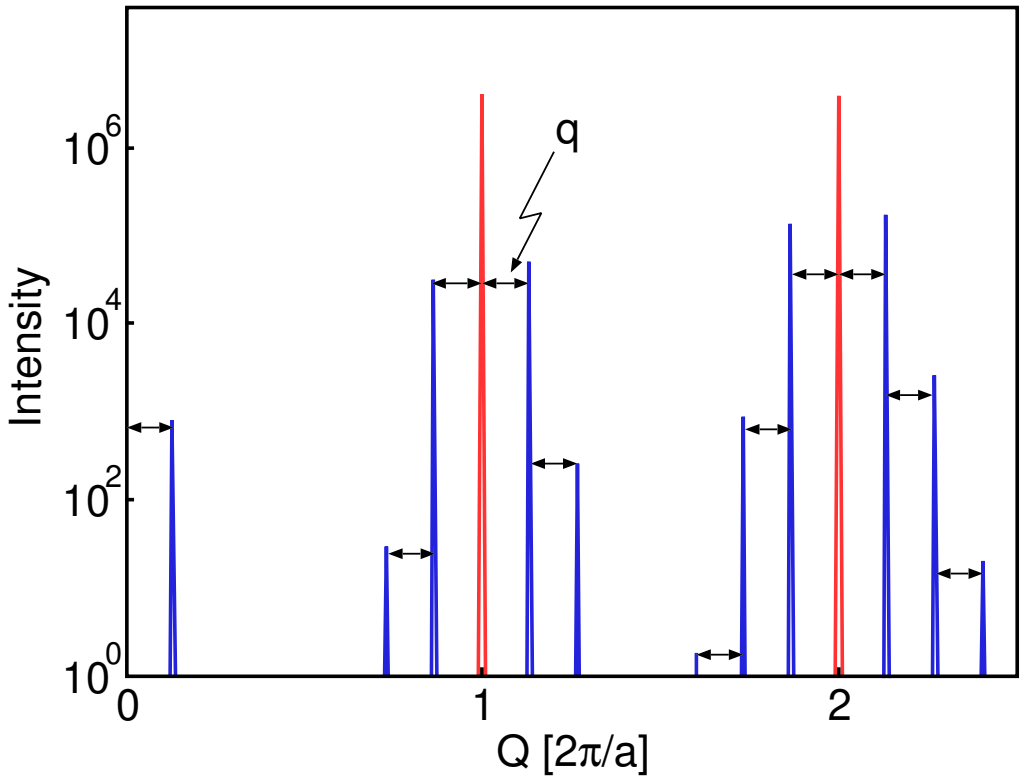

Quasicrystals

The only rotational symmetries which permit a space-filling lattice are 2-, 3-, 4-, and 6-fold.

Quasicrystals

The only rotational symmetries which permit a space-filling lattice are 2-, 3-, 4-, and 6-fold.

In 1984, D. Schechtman and co-workers reported the first observation of a "crystal" with long range order but no translational symmetry in rapidly cooled $Al_{86}Mn_{14}$.

Quasicrystals

The only rotational symmetries which permit a space-filling lattice are 2-, 3-, 4-, and 6-fold.

In 1984, D. Schechtman and co-workers reported the first observation of a "crystal" with long range order but no translational symmetry in rapidly cooled $Al_{86}Mn_{14}$.

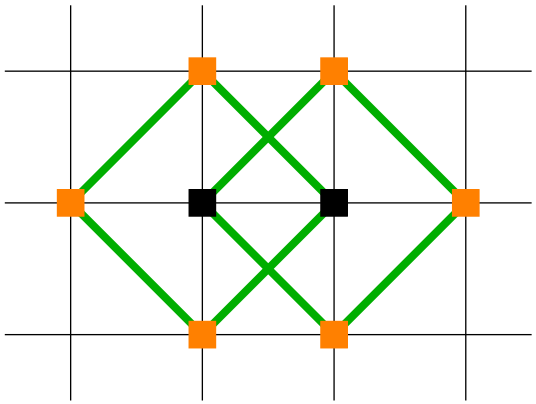

Quasicrystals

The only rotational symmetries which permit a space-filling lattice are 2-, 3-, 4-, and 6-fold.

In 1984, D. Schechtman and co-workers reported the first observation of a "crystal" with long range order but no translational symmetry in rapidly cooled $Al_{86}Mn_{14}$.

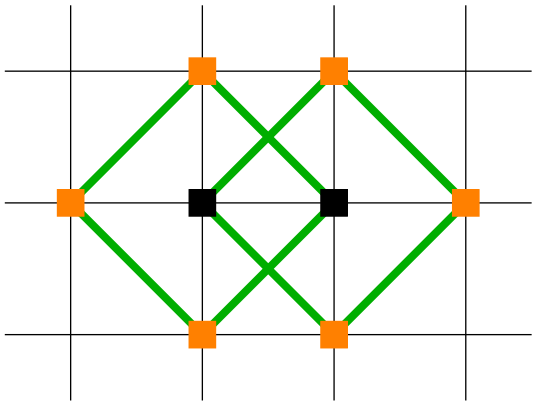

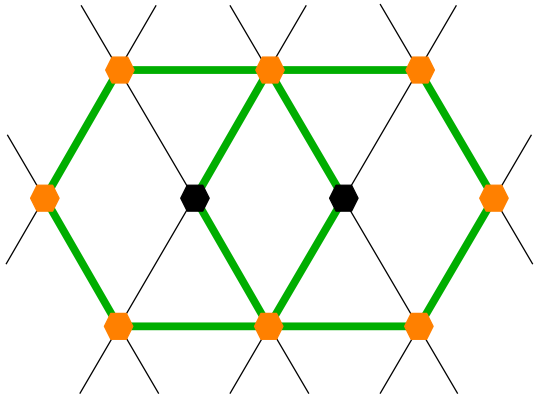

Quasicrystals

The only rotational symmetries which permit a space-filling lattice are 2-, 3-, 4-, and 6-fold.

In 1984, D. Schechtman and co-workers reported the first observation of a "crystal" with long range order but no translational symmetry in rapidly cooled $Al_{86}Mn_{14}$.

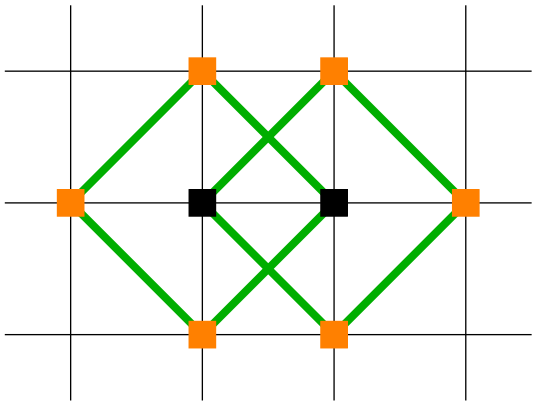

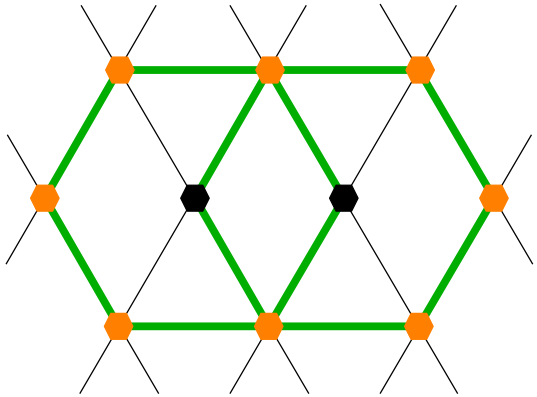

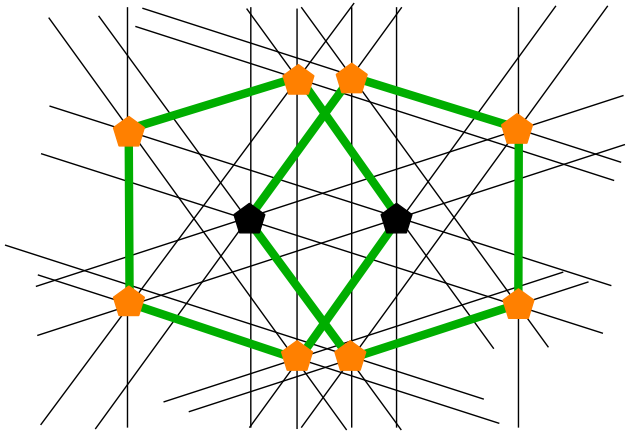

Quasicrystals

The only rotational symmetries which permit a space-filling lattice are 2-, 3-, 4-, and 6-fold.

In 1984, D. Schechtman and co-workers reported the first observation of a "crystal" with long range order but no translational symmetry in rapidly cooled $Al_{86}Mn_{14}$.

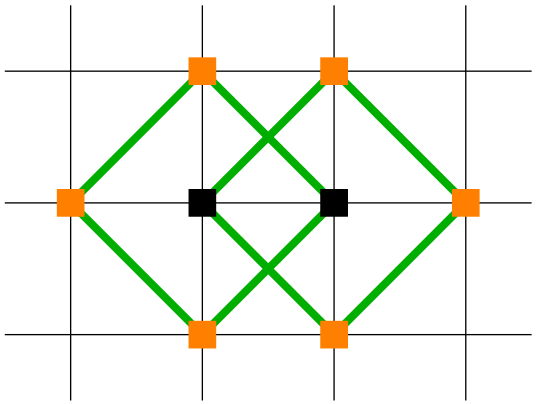
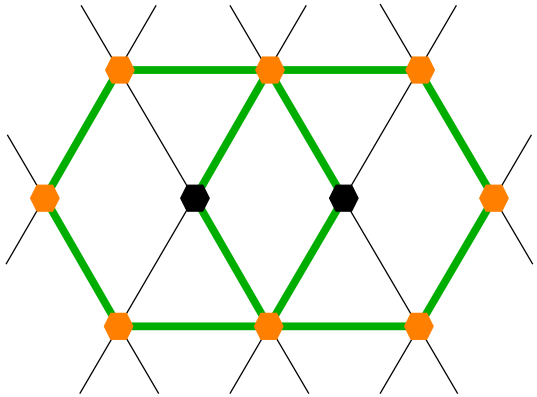
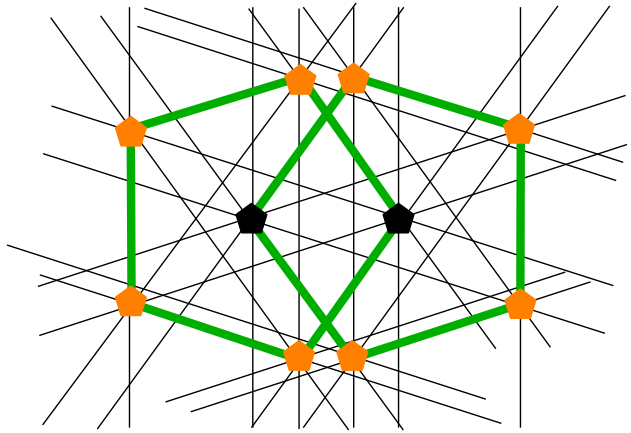

Initially this result was not accepted but as many new materials with the same were discovered it was clear that a new kind of crystal had been discovered.

Quasicrystals

The only rotational symmetries which permit a space-filling lattice are 2-, 3-, 4-, and 6-fold.

In 1984, D. Schechtman and co-workers reported the first observation of a "crystal" with long range order but no translational symmetry in rapidly cooled $Al_{86}Mn_{14}$.

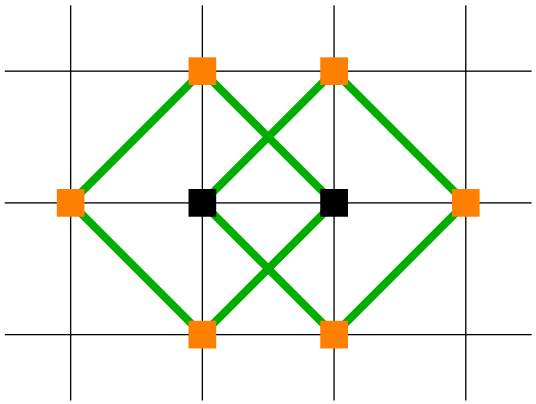
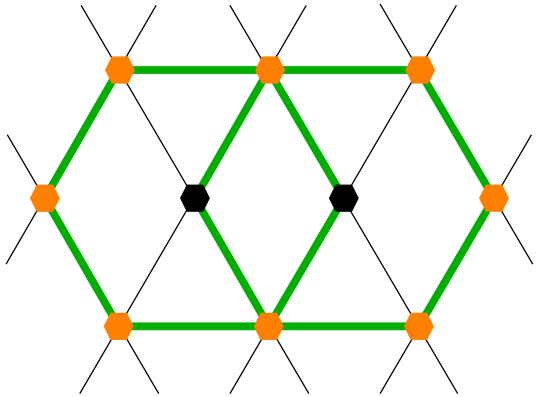
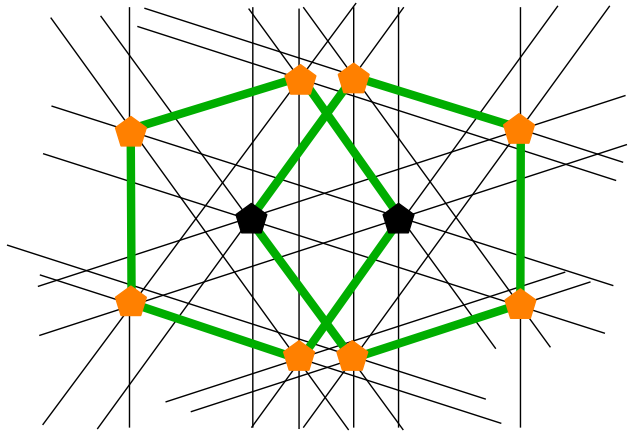

Initially this result was not accepted but as many new materials with the same were discovered it was clear that a new kind of crystal had been discovered.

In 2011 Shechtman was awarded the Nobel Prize in Chemistry

5-fold symmetry

The electron micrographs show that there must be long range order to be able to get such sharp diffraction peaks

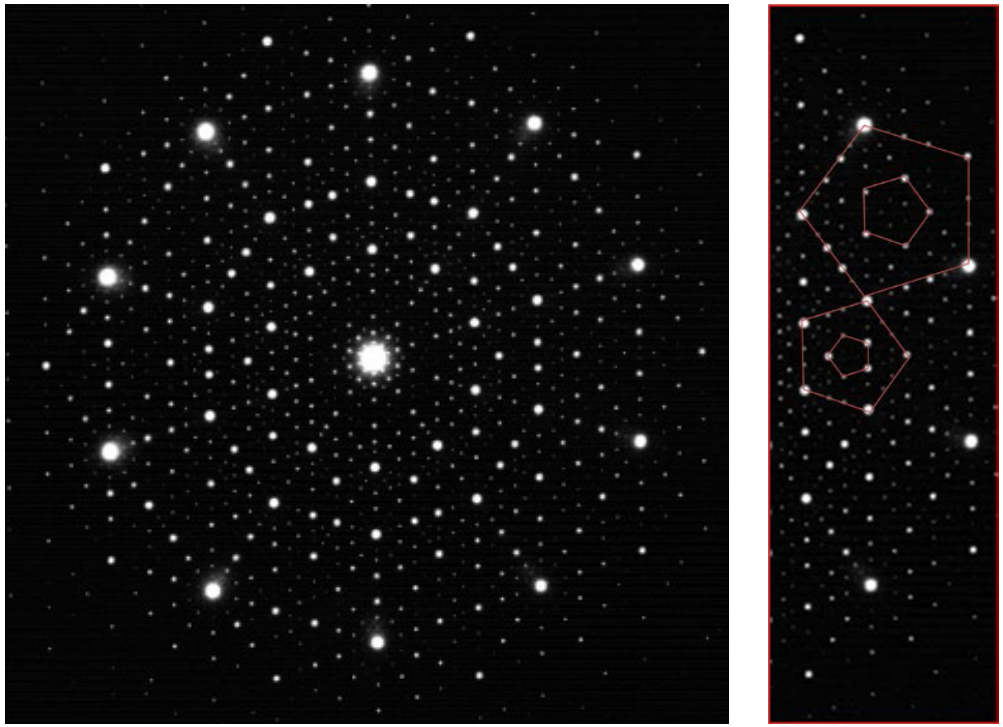

"Metallic phase with long-range orientational order and no translational symmetry," D. Shechtman, I. Blech, D. Gratias, and J.W. Cahn, *Phys. Rev. Lett.* **53**, 1951-1953 (1984)

5-fold symmetry

The electron micrographs show that there must be long range order to be able to get such sharp diffraction peaks

The 5-fold symmetry is evident in the 10 spots surrounding the center of the left image and the pentagonal arrangements of atoms in the image on the right.

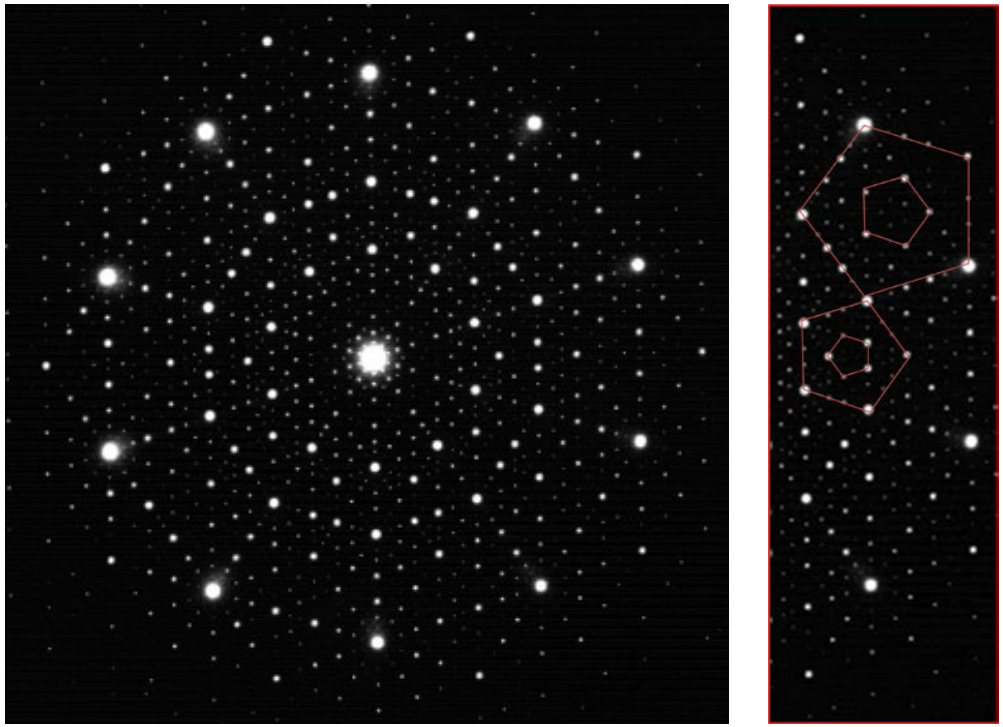

"Metallic phase with long-range orientational order and no translational symmetry," D. Shechtman, I. Blech, D. Gratias, and J.W. Cahn, *Phys. Rev. Lett.* **53**, 1951-1953 (1984)

5-fold symmetry

The electron micrographs show that there must be long range order to be able to get such sharp diffraction peaks

The 5-fold symmetry is evident in the 10 spots surrounding the center of the left image and the pentagonal arrangements of atoms in the image on the right.

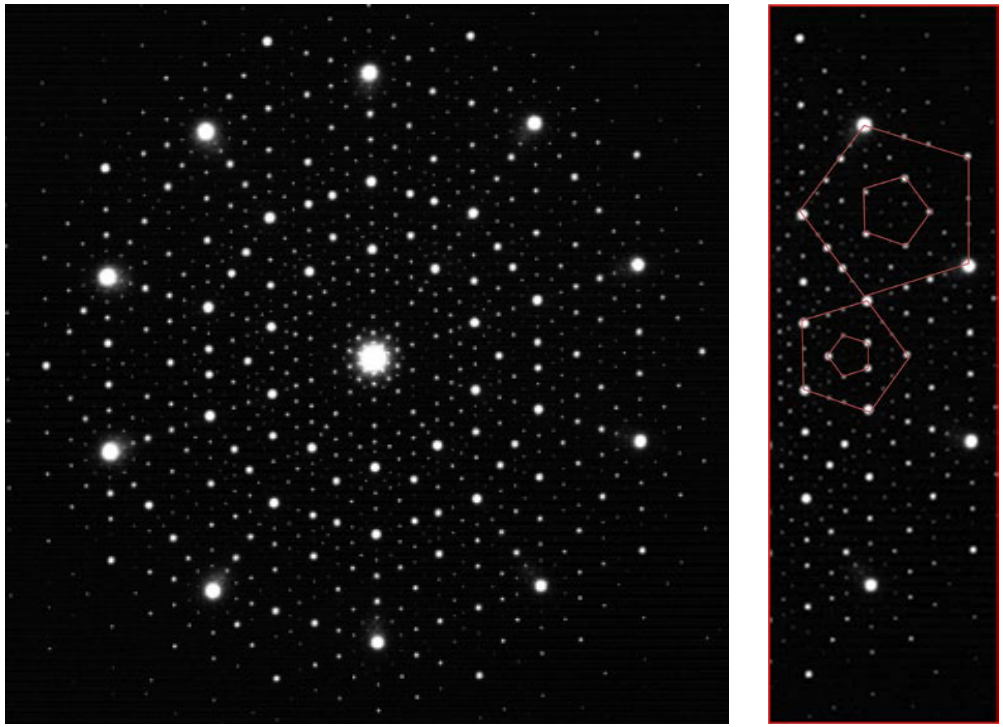

This metastable phase was also found with Fe and Cr in the place of Mn.

"Metallic phase with long-range orientational order and no translational symmetry," D. Shechtman, I. Blech, D. Gratias, and J.W. Cahn, *Phys. Rev. Lett.* **53**, 1951-1953 (1984)

5-fold symmetry

The electron micrographs show that there must be long range order to be able to get such sharp diffraction peaks

The 5-fold symmetry is evident in the 10 spots surrounding the center of the left image and the pentagonal arrangements of atoms in the image on the right.

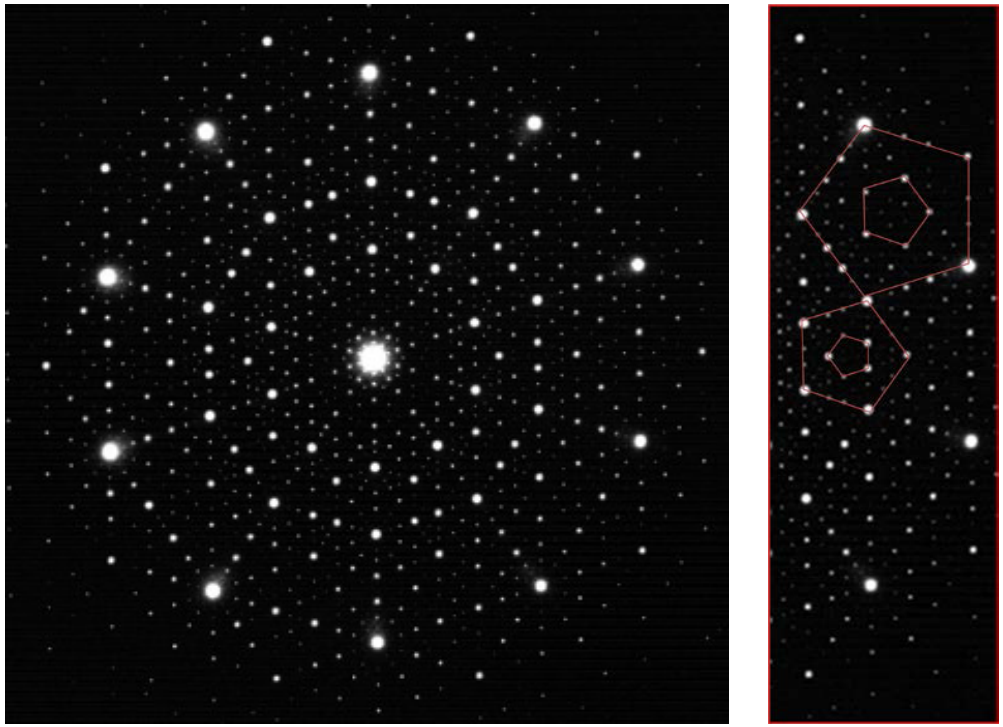

This metastable phase was also found with Fe and Cr in the place of Mn.

Other groups have discovered stable icosahedral phases with three and two elements.

"Metallic phase with long-range orientational order and no translational symmetry," D. Shechtman, I. Blech, D. Gratias, and J.W. Cahn, *Phys. Rev. Lett.* **53**, 1951-1953 (1984)

Quasicrystal diffraction patterns

The $Al_{65}Cu_{20}Fe_{15}$ system was one of the first stable quasicrystals to be discovered. Later discovery of stable quasicrystals in the Ta-Te, Cd-Ca, and Cd-Yb systems enabled large crystals to be grown.

"A stable quasicrystal in Al-Cu-Fe system," A.-P. Tsai, A. Inoue, and T. Masumoto, *Jap. J. Appl. Phys.* **26**, L1505 (1987)

Quasicrystal diffraction patterns

The $Al_{65}Cu_{20}Fe_{15}$ system was one of the first stable quasicrystals to be discovered. Later discovery of stable quasicrystals in the Ta-Te, Cd-Ca, and Cd-Yb systems enabled large crystals to be grown.

The diffraction pattern and SEM images show the hallmark of an icosahedral crystal

"A stable quasicrystal in Al-Cu-Fe system," A.-P. Tsai, A. Inoue, and T. Masumoto, *Jap. J. Appl. Phys.* **26**, L1505 (1987)

Quasicrystal diffraction patterns

The $Al_{65}Cu_{20}Fe_{15}$ system was one of the first stable quasicrystals to be discovered. Later discovery of stable quasicrystals in the Ta-Te, Cd-Ca, and Cd-Yb systems enabled large crystals to be grown.

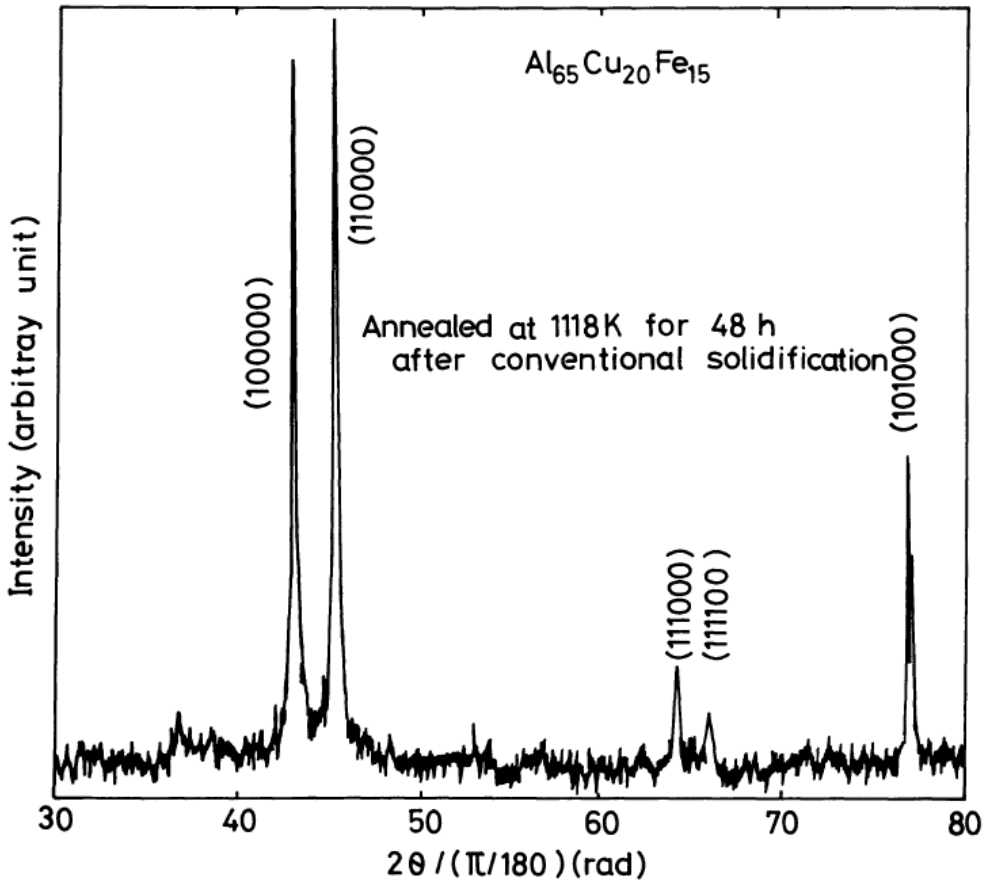

The diffraction pattern and SEM images show the hallmark of an icosahedral crystal

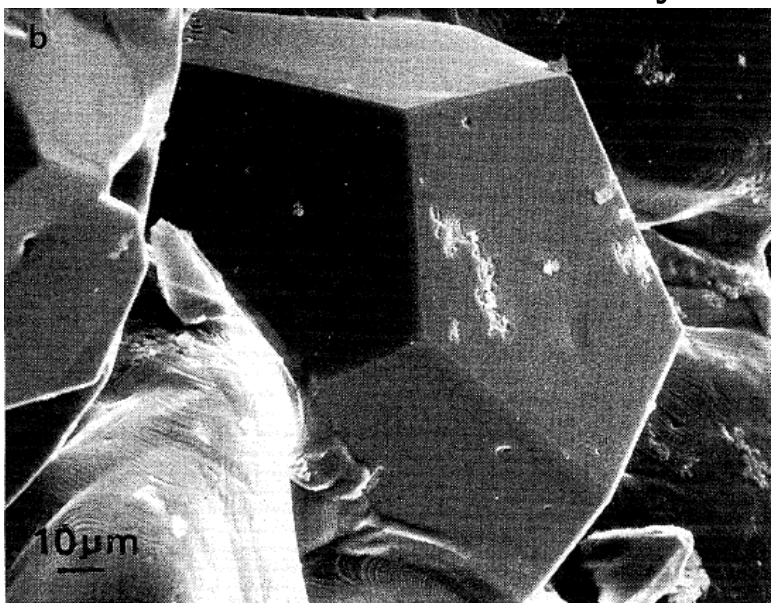

"A stable quasicrystal in Al-Cu-Fe system," A.-P. Tsai, A. Inoue, and T. Masumoto, *Jap. J. Appl. Phys.* **26**, L1505 (1987)

Lattice Vibrations

Atoms on a lattice are not rigid but vibrate. There is zero-point motion as well as thermal motion. These vibrations influence the x-ray scattering.

Lattice Vibrations

Atoms on a lattice are not rigid but vibrate. There is zero-point motion as well as thermal motion. These vibrations influence the x-ray scattering.

For a 1D lattice, we replace the position of the atom with its *instantaneous* position, $\vec{R}_n + \vec{u}_n$ where $\vec{u}_n$ is the displacement from the equilibrium position, $\vec{R}_n$.

Lattice Vibrations

Atoms on a lattice are not rigid but vibrate. There is zero-point motion as well as thermal motion. These vibrations influence the x-ray scattering.

For a 1D lattice, we replace the position of the atom with its *instantaneous* position, $\vec{R}_n + \vec{u}_n$ where $\vec{u}_n$ is the displacement from the equilibrium position, $\vec{R}_n$. Computing the intensity:

Lattice Vibrations

Atoms on a lattice are not rigid but vibrate. There is zero-point motion as well as thermal motion. These vibrations influence the x-ray scattering.

For a 1D lattice, we replace the position of the atom with its *instantaneous* position, $\vec{R}_n + \vec{u}_n$ where $\vec{u}_n$ is the displacement from the equilibrium position, $\vec{R}_n$. Computing the intensity:

$$I = \left\langle \sum_m f(\vec{Q}) e^{i\vec{Q}\cdot(\vec{R}_m+\vec{u}_m)} \sum_n f^*(\vec{Q}) e^{-i\vec{Q}\cdot(\vec{R}_n+\vec{u}_n)} \right\rangle$$

Lattice Vibrations

Atoms on a lattice are not rigid but vibrate. There is zero-point motion as well as thermal motion. These vibrations influence the x-ray scattering.

For a 1D lattice, we replace the position of the atom with its *instantaneous* position, $\vec{R}_n + \vec{u}_n$ where $\vec{u}_n$ is the displacement from the equilibrium position, $\vec{R}_n$. Computing the intensity:

$$
\begin{aligned}
I &= \left\langle \sum_m f(\vec{Q}) e^{i\vec{Q}\cdot(\vec{R}_m+\vec{u}_m)} \sum_n f^*(\vec{Q}) e^{-i\vec{Q}\cdot(\vec{R}_n+\vec{u}_n)} \right\rangle \\
&= \sum_m \sum_n f(\vec{Q}) f^*(\vec{Q}) e^{i\vec{Q}\cdot(\vec{R}_m-\vec{R}_n)} \left\langle e^{i\vec{Q}\cdot(\vec{u}_m-\vec{u}_n)} \right\rangle
\end{aligned}
$$

Lattice Vibrations

Atoms on a lattice are not rigid but vibrate. There is zero-point motion as well as thermal motion. These vibrations influence the x-ray scattering.

For a 1D lattice, we replace the position of the atom with its *instantaneous* position, $\vec{R}_n + \vec{u}_n$ where $\vec{u}_n$ is the displacement from the equilibrium position, $\vec{R}_n$. Computing the intensity:

$$I = \left\langle \sum_m f(\vec{Q}) e^{i\vec{Q}\cdot(\vec{R}_m+\vec{u}_m)} \sum_n f^*(\vec{Q}) e^{-i\vec{Q}\cdot(\vec{R}_n+\vec{u}_n)} \right\rangle$$
$$= \sum_m \sum_n f(\vec{Q}) f^*(\vec{Q}) e^{i\vec{Q}\cdot(\vec{R}_m-\vec{R}_n)} \left\langle e^{i\vec{Q}\cdot(\vec{u}_m-\vec{u}_n)} \right\rangle$$

The last term is a time average which can be simplified by first taking the scalar product, $\vec{Q}\cdot\vec{u}_n = u_{Qn}$ to project the displacement along the scattering vector, then applying the Baker-Hausdorff theorem, $\left\langle e^{ix} \right\rangle = e^{-\langle x^2 \rangle/2}$

Lattice Vibrations

Atoms on a lattice are not rigid but vibrate. There is zero-point motion as well as thermal motion. These vibrations influence the x-ray scattering.

For a 1D lattice, we replace the position of the atom with its *instantaneous* position, $\vec{R}_n + \vec{u}_n$ where $\vec{u}_n$ is the displacement from the equilibrium position, $\vec{R}_n$. Computing the intensity:

$$I = \left\langle \sum_m f(\vec{Q}) e^{i\vec{Q}\cdot(\vec{R}_m+\vec{u}_m)} \sum_n f^*(\vec{Q}) e^{-i\vec{Q}\cdot(\vec{R}_n+\vec{u}_n)} \right\rangle$$
$$= \sum_m \sum_n f(\vec{Q}) f^*(\vec{Q}) e^{i\vec{Q}\cdot(\vec{R}_m-\vec{R}_n)} \left\langle e^{i\vec{Q}\cdot(\vec{u}_m-\vec{u}_n)} \right\rangle$$

The last term is a time average which can be simplified by first taking the scalar product, $\vec{Q}\cdot\vec{u}_n = u_{Qn}$ to project the displacement along the scattering vector, then applying the Baker-Hausdorff theorem, $\left\langle e^{ix} \right\rangle = e^{-\langle x^2\rangle/2}$

$$\left\langle e^{i\vec{Q}\cdot(\vec{u}_m-\vec{u}_n)} \right\rangle = \left\langle e^{iQ(u_{Qm}-u_{Qn})} \right\rangle$$

Lattice Vibrations

Atoms on a lattice are not rigid but vibrate. There is zero-point motion as well as thermal motion. These vibrations influence the x-ray scattering.

For a 1D lattice, we replace the position of the atom with its *instantaneous* position, $\vec{R}_n + \vec{u}_n$ where $\vec{u}_n$ is the displacement from the equilibrium position, $\vec{R}_n$. Computing the intensity:

$$I = \left\langle \sum_m f(\vec{Q}) e^{i\vec{Q}\cdot(\vec{R}_m+\vec{u}_m)} \sum_n f^*(\vec{Q}) e^{-i\vec{Q}\cdot(\vec{R}_n+\vec{u}_n)} \right\rangle$$
$$= \sum_m \sum_n f(\vec{Q}) f^*(\vec{Q}) e^{i\vec{Q}\cdot(\vec{R}_m-\vec{R}_n)} \left\langle e^{i\vec{Q}\cdot(\vec{u}_m-\vec{u}_n)} \right\rangle$$

The last term is a time average which can be simplified by first taking the scalar product, $\vec{Q}\cdot\vec{u}_n = u_{Qn}$ to project the displacement along the scattering vector, then applying the Baker-Hausdorff theorem, $\left\langle e^{ix} \right\rangle = e^{-\langle x^2\rangle/2}$

$$\left\langle e^{i\vec{Q}\cdot(\vec{u}_m-\vec{u}_n)} \right\rangle = \left\langle e^{iQ(u_{Qm}-u_{Qn})} \right\rangle = e^{-\langle Q^2(u_{Qm}-u_{Qn})^2\rangle/2}$$

Lattice Vibrations

$$\left\langle e^{iQ(u_{Qm}-u_{Qn})} \right\rangle = e^{-Q^2\langle u_{Qm}^2\rangle/2} e^{-Q^2\langle u_{Qn}^2\rangle/2} e^{Q^2\langle u_{Qm}u_{Qn}\rangle}$$

Lattice Vibrations

$$\left\langle e^{iQ(u_{Qm}-u_{Qn})} \right\rangle = e^{-Q^2\langle u_{Qm}^2\rangle/2} e^{-Q^2\langle u_{Qn}^2\rangle/2} e^{Q^2\langle u_{Qm}u_{Qn}\rangle}$$

$$= e^{-Q^2\langle u_{Q}^2\rangle} e^{Q^2\langle u_{Qm}u_{Qn}\rangle}$$

Lattice Vibrations

$$\left\langle e^{iQ(u_{Qm}-u_{Qn})} \right\rangle = e^{-Q^2\langle u_{Qm}^2\rangle/2} e^{-Q^2\langle u_{Qn}^2\rangle/2} e^{Q^2\langle u_{Qm}u_{Qn}\rangle}$$

$$= e^{-Q^2\langle u_{Q}^2\rangle} e^{Q^2\langle u_{Qm}u_{Qn}\rangle} = e^{-2M} e^{Q^2\langle u_{Qm}u_{Qn}\rangle}$$

Lattice Vibrations

$$\left\langle e^{iQ(u_{Qm}-u_{Qn})} \right\rangle = e^{-Q^2\langle u_{Qm}^2\rangle/2} e^{-Q^2\langle u_{Qn}^2\rangle/2} e^{Q^2\langle u_{Qm}u_{Qn}\rangle}$$

$$= e^{-Q^2\langle u_Q^2\rangle} e^{Q^2\langle u_{Qm}u_{Qn}\rangle} = e^{-2M} e^{Q^2\langle u_{Qm}u_{Qn}\rangle}$$

$$= e^{-2M}\left[1 + e^{Q^2\langle u_{Qm}u_{Qn}\rangle} - 1\right]$$

Lattice Vibrations

$$\left\langle e^{iQ(u_{Qm}-u_{Qn})} \right\rangle = e^{-Q^2\langle u_{Qm}^2\rangle/2} e^{-Q^2\langle u_{Qn}^2\rangle/2} e^{Q^2\langle u_{Qm}u_{Qn}\rangle}$$

$$= e^{-Q^2\langle u_Q^2\rangle} e^{Q^2\langle u_{Qm}u_{Qn}\rangle} = e^{-2M} e^{Q^2\langle u_{Qm}u_{Qn}\rangle}$$

$$= e^{-2M}\left[1 + e^{Q^2\langle u_{Qm}u_{Qn}\rangle} - 1\right]$$

Substituting into the expression for intensity

Lattice Vibrations

$$\left\langle e^{iQ(u_{Qm}-u_{Qn})} \right\rangle = e^{-Q^2\langle u_{Qm}^2\rangle/2} e^{-Q^2\langle u_{Qn}^2\rangle/2} e^{Q^2\langle u_{Qm}u_{Qn}\rangle}$$

$$= e^{-Q^2\langle u_{Q}^2\rangle} e^{Q^2\langle u_{Qm}u_{Qn}\rangle} = e^{-2M} e^{Q^2\langle u_{Qm}u_{Qn}\rangle}$$

$$= e^{-2M}\left[1 + e^{Q^2\langle u_{Qm}u_{Qn}\rangle} - 1\right]$$

Substituting into the expression for intensity

$$I = \sum_m \sum_n f(\vec{Q}) e^{-M} e^{i\vec{Q}\cdot\vec{R}_m} f^*(\vec{Q}) e^{-M} e^{-i\vec{Q}\cdot\vec{R}_n}$$

$$+ \sum_m \sum_n f(\vec{Q}) e^{-M} e^{i\vec{Q}\cdot\vec{R}_m} f^*(\vec{Q}) e^{-M} e^{-i\vec{Q}\cdot\vec{R}_n} \left[e^{Q^2\langle u_{Qm}u_{Qn}\rangle} - 1\right]$$

Lattice Vibrations

$$\left\langle e^{iQ(u_{Qm}-u_{Qn})} \right\rangle = e^{-Q^2\langle u_{Qm}^2\rangle/2} e^{-Q^2\langle u_{Qn}^2\rangle/2} e^{Q^2\langle u_{Qm}u_{Qn}\rangle}$$

$$= e^{-Q^2\langle u_Q^2\rangle} e^{Q^2\langle u_{Qm}u_{Qn}\rangle} = e^{-2M} e^{Q^2\langle u_{Qm}u_{Qn}\rangle}$$

$$= e^{-2M}\left[1 + e^{Q^2\langle u_{Qm}u_{Qn}\rangle} - 1\right]$$

Substituting into the expression for intensity

$$I = \sum_m \sum_n f(\vec{Q}) e^{-M} e^{i\vec{Q}\cdot\vec{R}_m} f^*(\vec{Q}) e^{-M} e^{-i\vec{Q}\cdot\vec{R}_n}$$

$$+ \sum_m \sum_n f(\vec{Q}) e^{-M} e^{i\vec{Q}\cdot\vec{R}_m} f^*(\vec{Q}) e^{-M} e^{-i\vec{Q}\cdot\vec{R}_n} \left[e^{Q^2\langle u_{Qm}u_{Qn}\rangle} - 1\right]$$

The first term is just the elastic scattering from the lattice with the addition of the term $e^{-M} = e^{-Q^2\langle u_Q^2\rangle/2}$, called the Debye-Waller factor.

Lattice Vibrations

$$\left\langle e^{iQ(u_{Qm}-u_{Qn})} \right\rangle = e^{-Q^2\langle u_{Qm}^2\rangle/2} e^{-Q^2\langle u_{Qn}^2\rangle/2} e^{Q^2\langle u_{Qm}u_{Qn}\rangle}$$

$$= e^{-Q^2\langle u_Q^2\rangle} e^{Q^2\langle u_{Qm}u_{Qn}\rangle} = e^{-2M} e^{Q^2\langle u_{Qm}u_{Qn}\rangle}$$

$$= e^{-2M}\left[1 + e^{Q^2\langle u_{Qm}u_{Qn}\rangle} - 1\right]$$

Substituting into the expression for intensity

$$I = \sum_m \sum_n f(\vec{Q}) e^{-M} e^{i\vec{Q}\cdot\vec{R}_m} f^*(\vec{Q}) e^{-M} e^{-i\vec{Q}\cdot\vec{R}_n}$$

$$+ \sum_m \sum_n f(\vec{Q}) e^{-M} e^{i\vec{Q}\cdot\vec{R}_m} f^*(\vec{Q}) e^{-M} e^{-i\vec{Q}\cdot\vec{R}_n} \left[e^{Q^2\langle u_{Qm}u_{Qn}\rangle} - 1\right]$$

The first term is just the elastic scattering from the lattice with the addition of the term $e^{-M} = e^{-Q^2\langle u_Q^2\rangle/2}$, called the Debye-Waller factor.

The second term is the Thermal Diffuse Scattering and actually increases with mean squared displacement.

Thermal Diffuse Scattering

$$I^{TDS} = \sum_m \sum_n f(\vec{Q}) e^{-M} e^{i\vec{Q}\cdot\vec{R}_m} f^*(\vec{Q}) e^{-M} e^{-i\vec{Q}\cdot\vec{R}_n} \left[e^{Q^2 \langle u_{Qm} u_{Qn} \rangle} - 1 \right]$$

Thermal Diffuse Scattering

$$I^{TDS} = \sum_m \sum_n f(\vec{Q}) e^{-M} e^{i\vec{Q}\cdot\vec{R}_m} f^*(\vec{Q}) e^{-M} e^{-i\vec{Q}\cdot\vec{R}_n} \left[e^{Q^2 \langle u_{Qm} u_{Qn} \rangle} - 1 \right]$$

The TDS has a width determined by the correlated displacement of atoms which is much broader than a Bragg peak.

Thermal Diffuse Scattering

$$I^{TDS} = \sum_m \sum_n f(\vec{Q}) e^{-M} e^{i\vec{Q}\cdot\vec{R}_m} f^*(\vec{Q}) e^{-M} e^{-i\vec{Q}\cdot\vec{R}_n} \left[e^{Q^2 \langle u_{Qm} u_{Qn} \rangle} - 1 \right]$$

The TDS has a width determined by the correlated displacement of atoms which is much broader than a Bragg peak.

These correlated motions are just phonons.

Thermal Diffuse Scattering

$$I^{TDS} = \sum_m \sum_n f(\vec{Q}) e^{-M} e^{i\vec{Q}\cdot\vec{R}_m} f^*(\vec{Q}) e^{-M} e^{-i\vec{Q}\cdot\vec{R}_n} \left[e^{Q^2 \langle u_{Qm} u_{Qn} \rangle} - 1 \right]$$

The TDS has a width determined by the correlated displacement of atoms which is much broader than a Bragg peak.

These correlated motions are just phonons.

A 0.5mm Si wafer illuminated by 28keV x-rays from an APS undulator were used to measure the phonon dispersion curves of silicon

Thermal Diffuse Scattering

$$I^{TDS} = \sum_m \sum_n f(\vec{Q}) e^{-M} e^{i\vec{Q}\cdot\vec{R}_m} f^*(\vec{Q}) e^{-M} e^{-i\vec{Q}\cdot\vec{R}_n} \left[e^{Q^2 \langle u_{Qm} u_{Qn} \rangle} - 1 \right]$$

The TDS has a width determined by the correlated displacement of atoms which is much broader than a Bragg peak.

These correlated motions are just phonons.

A 0.5mm Si wafer illuminated by 28keV x-rays from an APS undulator were used to measure the phonon dispersion curves of silicon

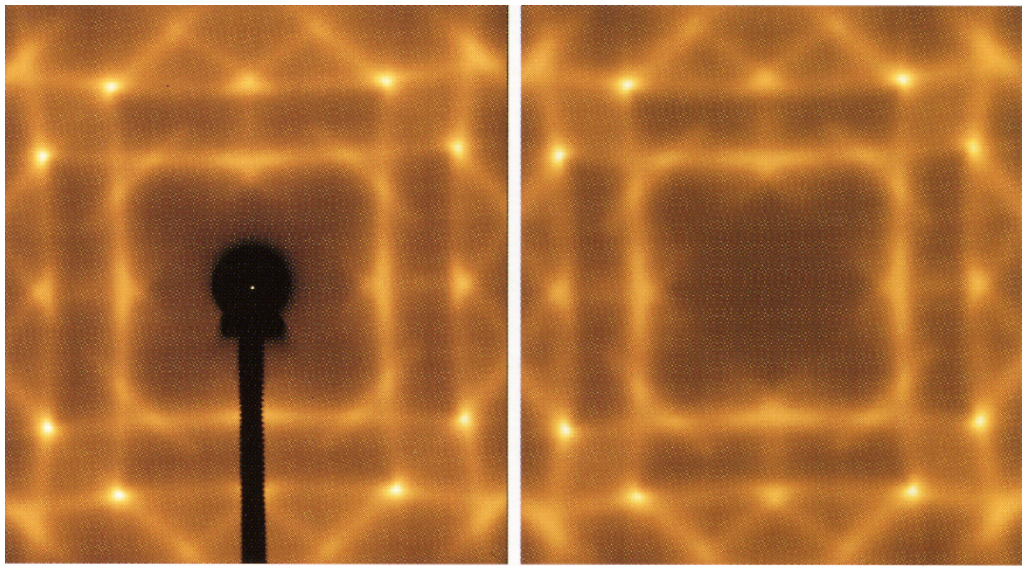

incident beam along (100)

M. Holt, et al. *Phys. Rev. Lett.* **83**, 3317 (1999).

Thermal Diffuse Scattering

$$I^{TDS} = \sum_m \sum_n f(\vec{Q}) e^{-M} e^{i\vec{Q}\cdot\vec{R}_m} f^*(\vec{Q}) e^{-M} e^{-i\vec{Q}\cdot\vec{R}_n} \left[e^{Q^2 \langle u_{Qm} u_{Qn} \rangle} - 1 \right]$$

The TDS has a width determined by the correlated displacement of atoms which is much broader than a Bragg peak.

These correlated motions are just phonons.

A 0.5mm Si wafer illuminated by 28keV x-rays from an APS undulator were used to measure the phonon dispersion curves of silicon

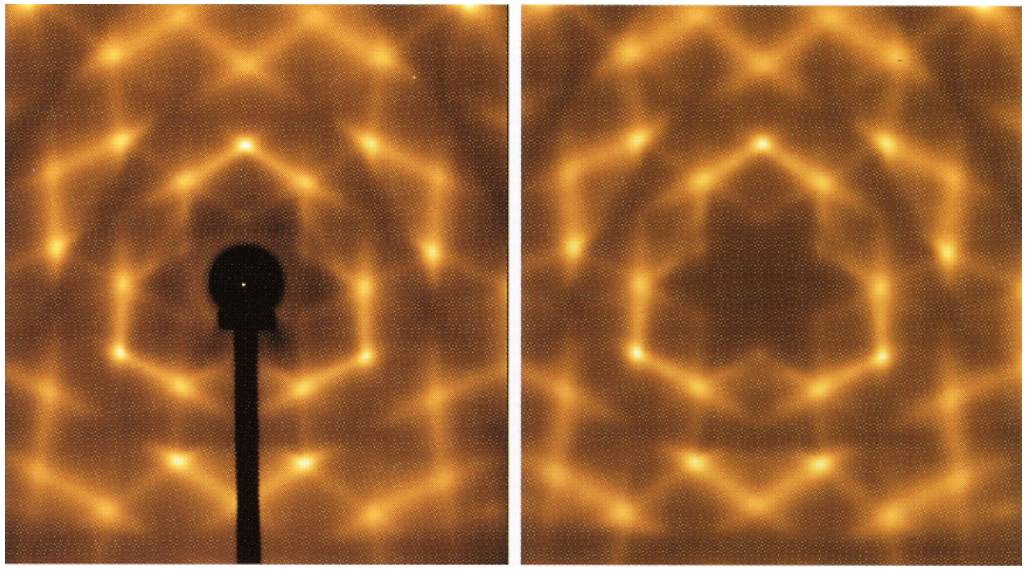

incident beam along (111)

M. Holt, et al. *Phys. Rev. Lett.* **83**, 3317 (1999).

Thermal Diffuse Scattering

$$I^{TDS} = \sum_m \sum_n f(\vec{Q}) e^{-M} e^{i\vec{Q}\cdot\vec{R}_m} f^*(\vec{Q}) e^{-M} e^{-i\vec{Q}\cdot\vec{R}_n} \left[e^{Q^2 \langle u_{Qm} u_{Qn} \rangle} - 1 \right]$$

The TDS has a width determined by the correlated displacement of atoms which is much broader than a Bragg peak.

These correlated motions are just phonons.

A 0.5mm Si wafer illuminated by 28keV x-rays from an APS undulator were used to measure the phonon dispersion curves of silicon

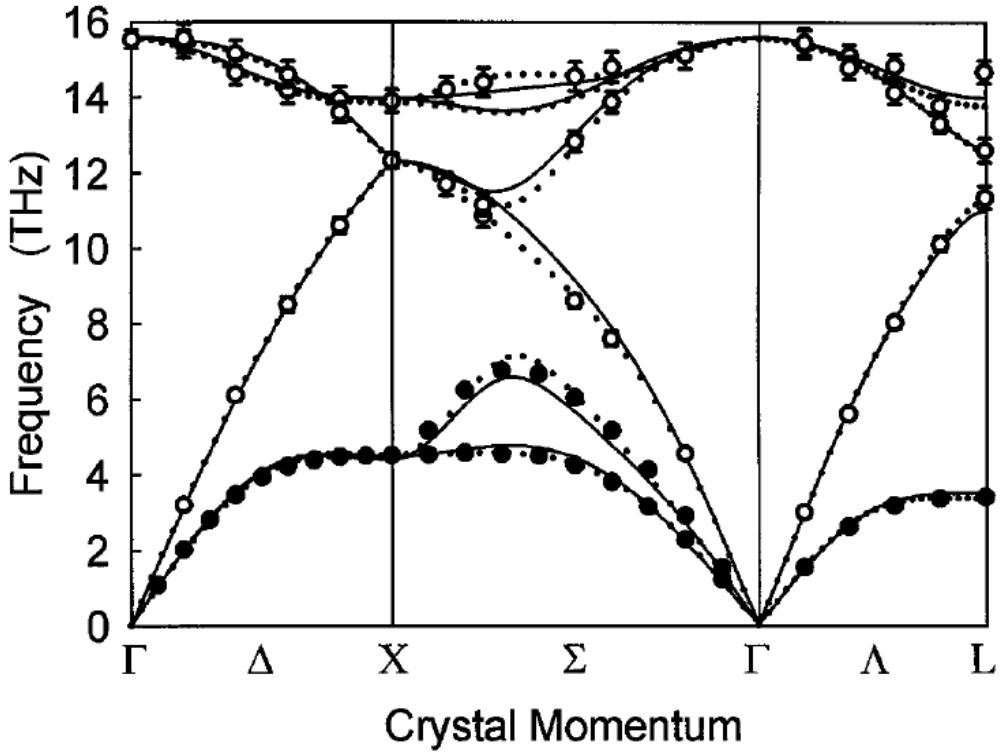

dotted line from this measurement

M. Holt, et al. *Phys. Rev. Lett.* **83**, 3317 (1999).

Properties of the Debye-Waller Factor

For crystals with several different types of atoms, we generalize the unit cell scattering factor.

Properties of the Debye-Waller Factor

For crystals with several different types of atoms, we generalize the unit cell scattering factor.

$$F^{u.c.} = \sum_j f_j(\vec{Q}) e^{-M_j} e^{i\vec{Q}\cdot\vec{r}_j}$$

Properties of the Debye-Waller Factor

For crystals with several different types of atoms, we generalize the unit cell scattering factor.

$$F^{u.c.} = \sum_j f_j(\vec{Q}) e^{-M_j} e^{i\vec{Q}\cdot\vec{r}_j}$$

$$M_j = \frac{1}{2} Q^2 \langle u_{Qj}^2 \rangle$$

Properties of the Debye-Waller Factor

For crystals with several different types of atoms, we generalize the unit cell scattering factor.

$$F^{u.c.} = \sum_j f_j(\vec{Q}) e^{-M_j} e^{i\vec{Q}\cdot\vec{r}_j}$$

$$M_j = \frac{1}{2} Q^2 \langle u_{Qj}^2 \rangle$$

$$= \frac{1}{2} \left(\frac{4\pi}{\lambda} \right)^2 \sin^2\theta \langle u_{Qj}^2 \rangle$$

Properties of the Debye-Waller Factor

For crystals with several different types of atoms, we generalize the unit cell scattering factor.

$$B_T^j = 8\pi^2 \langle u_{Qj}^2 \rangle$$

$$F^{u.c.} = \sum_j f_j(\vec{Q}) e^{-M_j} e^{i\vec{Q}\cdot\vec{r}_j}$$

$$M_j = \frac{1}{2} Q^2 \langle u_{Qj}^2 \rangle$$

$$= \frac{1}{2} \left(\frac{4\pi}{\lambda} \right)^2 \sin^2\theta \langle u_{Qj}^2 \rangle$$

$$M_j = B_T^j \left(\frac{\sin\theta}{\lambda} \right)^2$$

Properties of the Debye-Waller Factor

For crystals with several different types of atoms, we generalize the unit cell scattering factor.

$$B_T^j = 8\pi^2 \langle u_{Qj}^2 \rangle$$

for isotropic atomic vibrations

$$\begin{aligned} \langle u^2 \rangle &= \langle u_x^2 + u_y^2 + u_z^2 \rangle \\ &= 3\langle u_x^2 \rangle = 3\langle u_Q^2 \rangle \end{aligned}$$

$$F^{u.c.} = \sum_j f_j(\vec{Q}) e^{-M_j} e^{i\vec{Q}\cdot\vec{r}_j}$$

$$\begin{aligned} M_j &= \frac{1}{2} Q^2 \langle u_{Qj}^2 \rangle \\ &= \frac{1}{2} \left(\frac{4\pi}{\lambda} \right)^2 \sin^2\theta \langle u_{Qj}^2 \rangle \end{aligned}$$

$$M_j = B_T^j \left(\frac{\sin\theta}{\lambda} \right)^2$$

Properties of the Debye-Waller Factor

For crystals with several different types of atoms, we generalize the unit cell scattering factor.

$$B_T^j = 8\pi^2 \langle u_{Qj}^2 \rangle$$

for isotropic atomic vibrations

$$\begin{aligned} \langle u^2 \rangle &= \langle u_x^2 + u_y^2 + u_z^2 \rangle \\ &= 3\langle u_x^2 \rangle = 3\langle u_Q^2 \rangle \end{aligned}$$

$$F^{u.c.} = \sum_j f_j(\vec{Q}) e^{-M_j} e^{i\vec{Q}\cdot\vec{r}_j}$$

$$\begin{aligned} M_j &= \frac{1}{2} Q^2 \langle u_{Qj}^2 \rangle \\ &= \frac{1}{2} \left(\frac{4\pi}{\lambda} \right)^2 \sin^2\theta \langle u_{Qj}^2 \rangle \end{aligned}$$

$$M_j = B_T^j \left(\frac{\sin\theta}{\lambda} \right)^2$$

$$B_T^{iso} = \frac{8\pi^2}{3} \langle u^2 \rangle$$

Properties of the Debye-Waller Factor

For crystals with several different types of atoms, we generalize the unit cell scattering factor.

$$B_T^j = 8\pi^2 \langle u_{Qj}^2 \rangle$$

for isotropic atomic vibrations

$$\begin{aligned} \langle u^2 \rangle &= \langle u_x^2 + u_y^2 + u_z^2 \rangle \\ &= 3\langle u_x^2 \rangle = 3\langle u_Q^2 \rangle \end{aligned}$$

$$F^{u.c.} = \sum_j f_j(\vec{Q}) e^{-M_j} e^{i\vec{Q}\cdot\vec{r}_j}$$

$$\begin{aligned} M_j &= \frac{1}{2} Q^2 \langle u_{Qj}^2 \rangle \\ &= \frac{1}{2} \left(\frac{4\pi}{\lambda} \right)^2 \sin^2\theta \langle u_{Qj}^2 \rangle \end{aligned}$$

$$M_j = B_T^j \left(\frac{\sin\theta}{\lambda} \right)^2$$

$$B_T^{iso} = \frac{8\pi^2}{3} \langle u^2 \rangle$$

In general, Debye-Waller factors can be anisotropic

The Debye Model

The Debye model can be used to compute B_T by integrating a linear phonon dispersion relation up to a cutoff frequency, ω_D, called the Debye frequency.

The Debye Model

The Debye model can be used to compute B_T by integrating a linear phonon dispersion relation up to a cutoff frequency, ω_D, called the Debye frequency.

B_T is given as a function of the Debye temperature Θ.

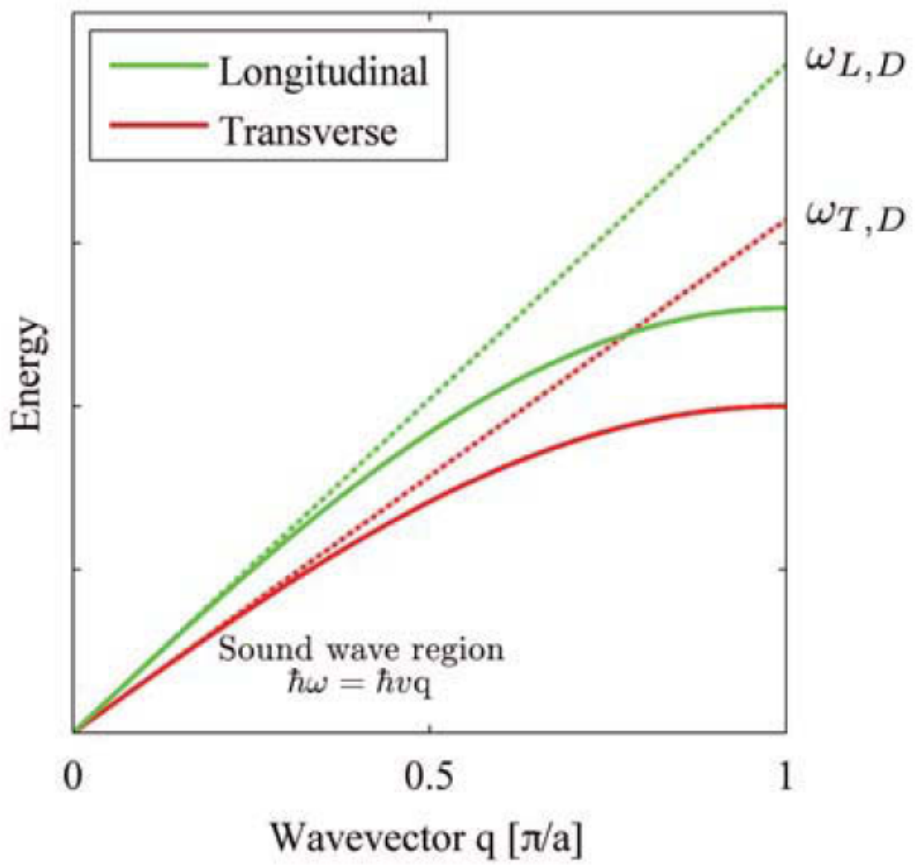

The Debye Model

The Debye model can be used to compute B_T by integrating a linear phonon dispersion relation up to a cutoff frequency, ω_D, called the Debye frequency.

B_T is given as a function of the Debye temperature Θ.

$$B_T = \frac{6h^2}{m_A k_B \Theta}\left[\frac{\phi(\Theta/T)}{\Theta/T} + \frac{1}{4}\right]$$

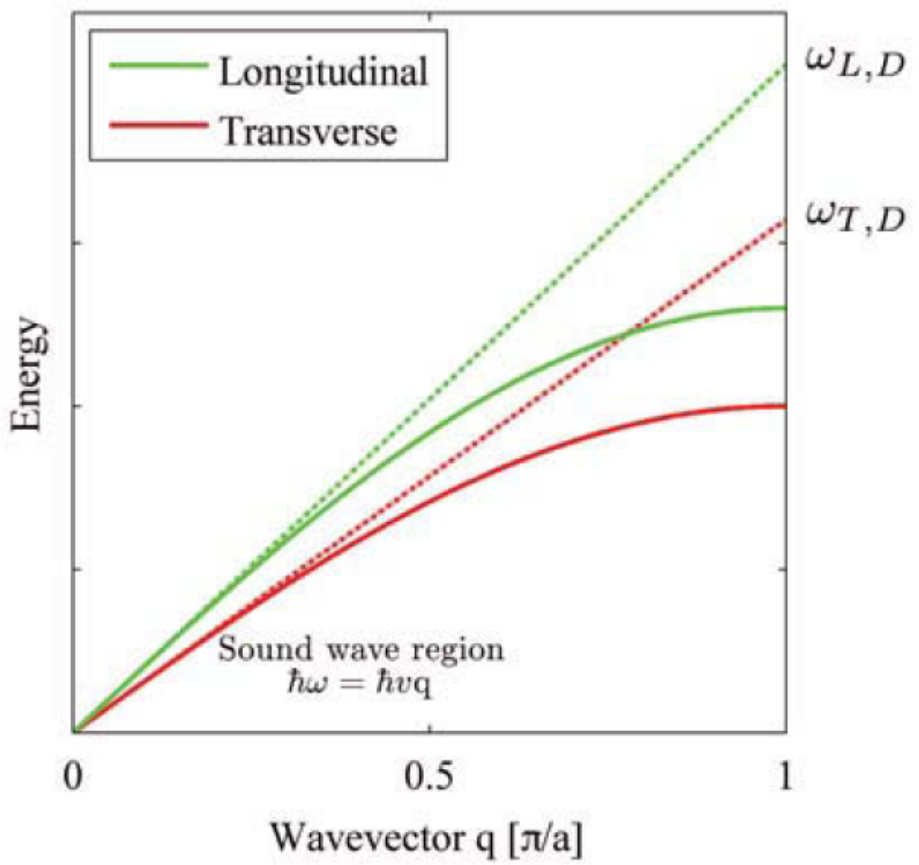

The Debye Model

The Debye model can be used to compute B_T by integrating a linear phonon dispersion relation up to a cutoff frequency, ω_D, called the Debye frequency.

B_T is given as a function of the Debye temperature Θ.

$$B_T = \frac{6h^2}{m_A k_B \Theta}\left[\frac{\phi(\Theta/T)}{\Theta/T} + \frac{1}{4}\right]$$

$$\phi(x) = \frac{1}{x}\int_0^{\Theta/T} \frac{\xi}{e^{\xi}-1} d\xi$$

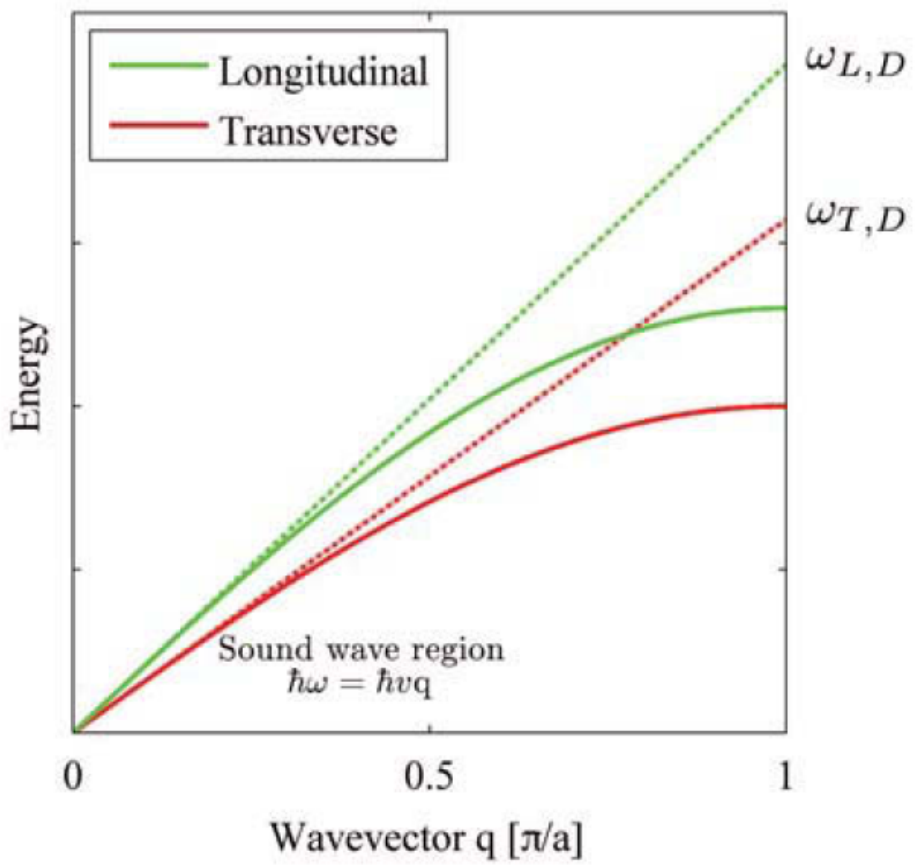

The Debye Model

The Debye model can be used to compute B_T by integrating a linear phonon dispersion relation up to a cutoff frequency, ω_D, called the Debye frequency.

B_T is given as a function of the Debye temperature Θ.

$$B_T = \frac{6h^2}{m_A k_B \Theta}\left[\frac{\phi(\Theta/T)}{\Theta/T} + \frac{1}{4}\right]$$

$$\phi(x) = \frac{1}{x}\int_0^{\Theta/T} \frac{\xi}{e^{\xi}-1} d\xi$$

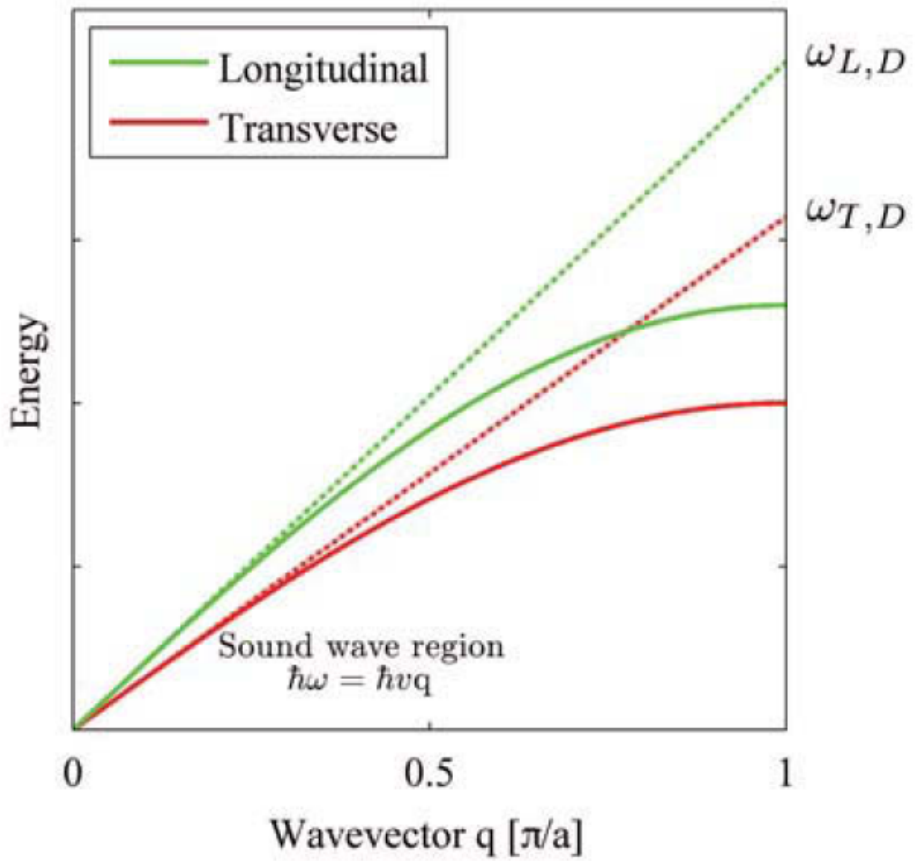

$$B_T[\text{Å}^2] = \frac{11492\text{T[K]}}{\text{A}\Theta^2[\text{K}^2]}\phi(\Theta/\text{T}) + \frac{2873}{\text{A}\Theta[\text{K}]}$$

Debye Temperatures

$$B_T = \frac{11492\,T}{A\Theta^2}\phi(\Theta/T) + \frac{2873}{A\Theta}$$

	A	Θ (K)	$B_{4.2}$	B_{77} (Å^2)	B_{293}
C*	12	2230	0.11	0.11	0.12
Al	27	428	0.25	0.30	0.72
Cu	63.5	343	0.13	0.17	0.47

*diamond

Debye Temperatures

$$B_T = \frac{11492\,T}{A\Theta^2}\phi(\Theta/T) + \frac{2873}{A\Theta}$$

diamond is very stiff and Θ does not vary much with temperature

	A	Θ (K)	$B_{4.2}$	B_{77} (Å^2)	B_{293}
C*	12	2230	0.11	0.11	0.12
Al	27	428	0.25	0.30	0.72
Cu	63.5	343	0.13	0.17	0.47

*diamond

Debye Temperatures

$$B_T = \frac{11492\,T}{A\Theta^2}\phi(\Theta/T) + \frac{2873}{A\Theta}$$

diamond is very stiff and Θ does not vary much with temperature

copper has a much lower Debye temperature and a wider variation of thermal factor with temperature

	A	Θ (K)	$B_{4.2}$	B_{77} (Å^2)	B_{293}
C*	12	2230	0.11	0.11	0.12
Al	27	428	0.25	0.30	0.72
Cu	63.5	343	0.13	0.17	0.47

*diamond

Debye Temperatures

$$B_T = \frac{11492\,T}{A\Theta^2}\phi(\Theta/T) + \frac{2873}{A\Theta}$$

diamond is very stiff and Θ does not vary much with temperature

copper has a much lower Debye temperature and a wider variation of thermal factor with temperature

	A	Θ (K)	$B_{4.2}$	B_{77} (Å^2)	B_{293}
C*	12	2230	0.11	0.11	0.12
Al	27	428	0.25	0.30	0.72
Cu	63.5	343	0.13	0.17	0.47

*diamond

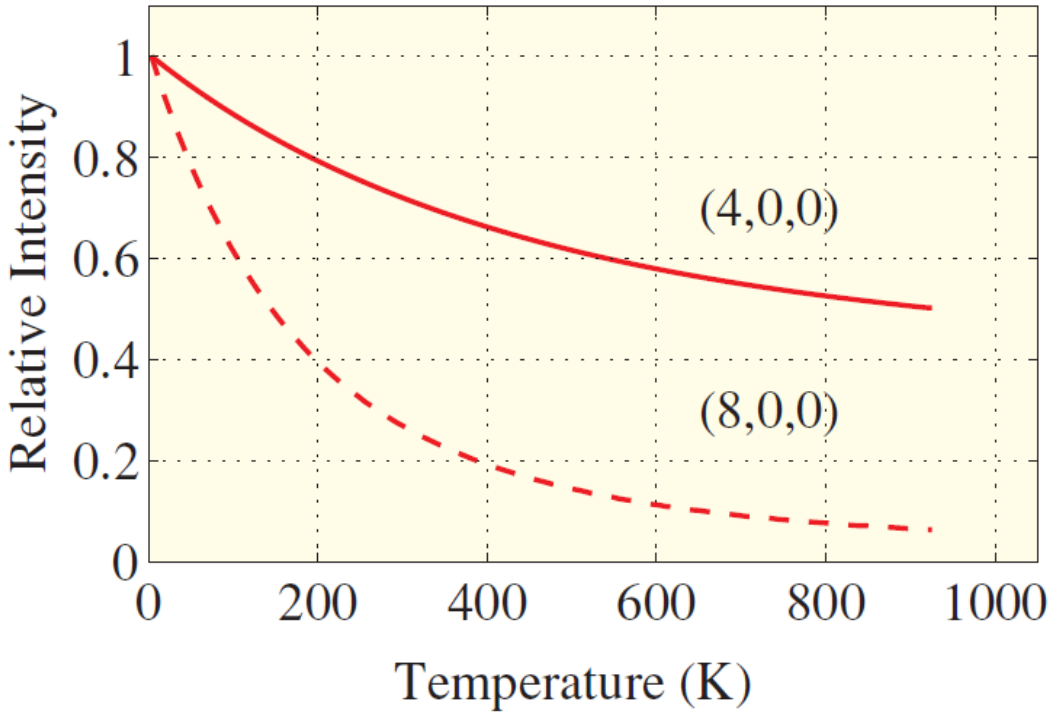

Powder diffraction

(a) Ambient pressure

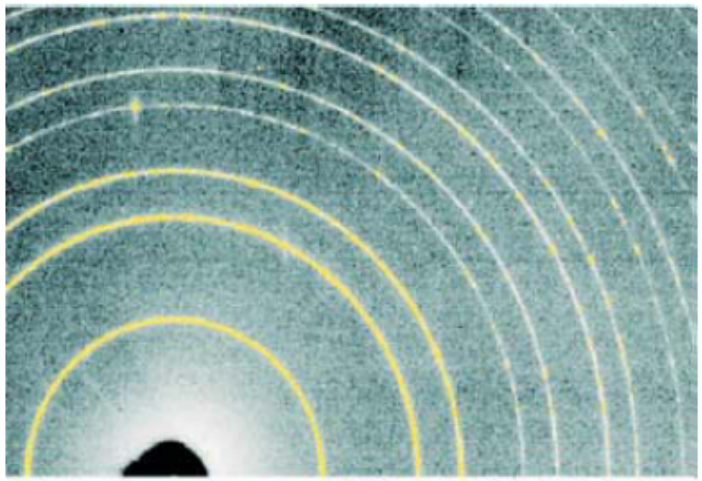

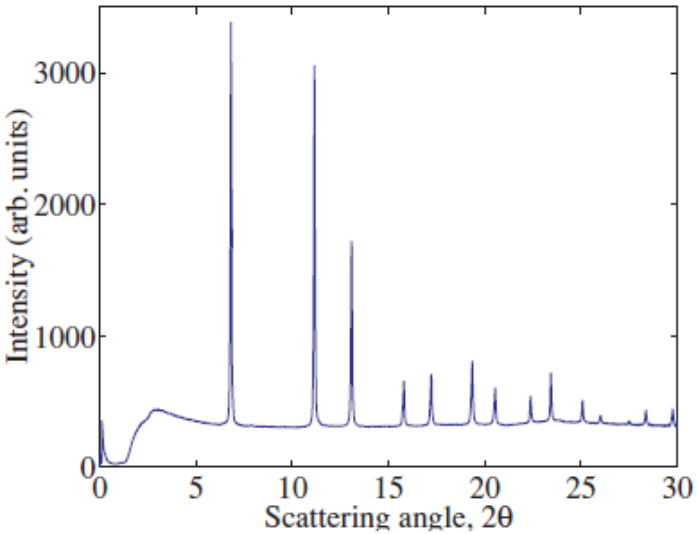

(b) 4.9 GPa (49 kbar)